USGS
science for a changing world

In cooperation with Pinnacle Mapping Technologies, Inc. and Northern Arizona University

A Vegetation Database for the Colorado River Ecosystem from Glen Canyon Dam to the Western Boundary of Grand Canyon National Park, Arizona

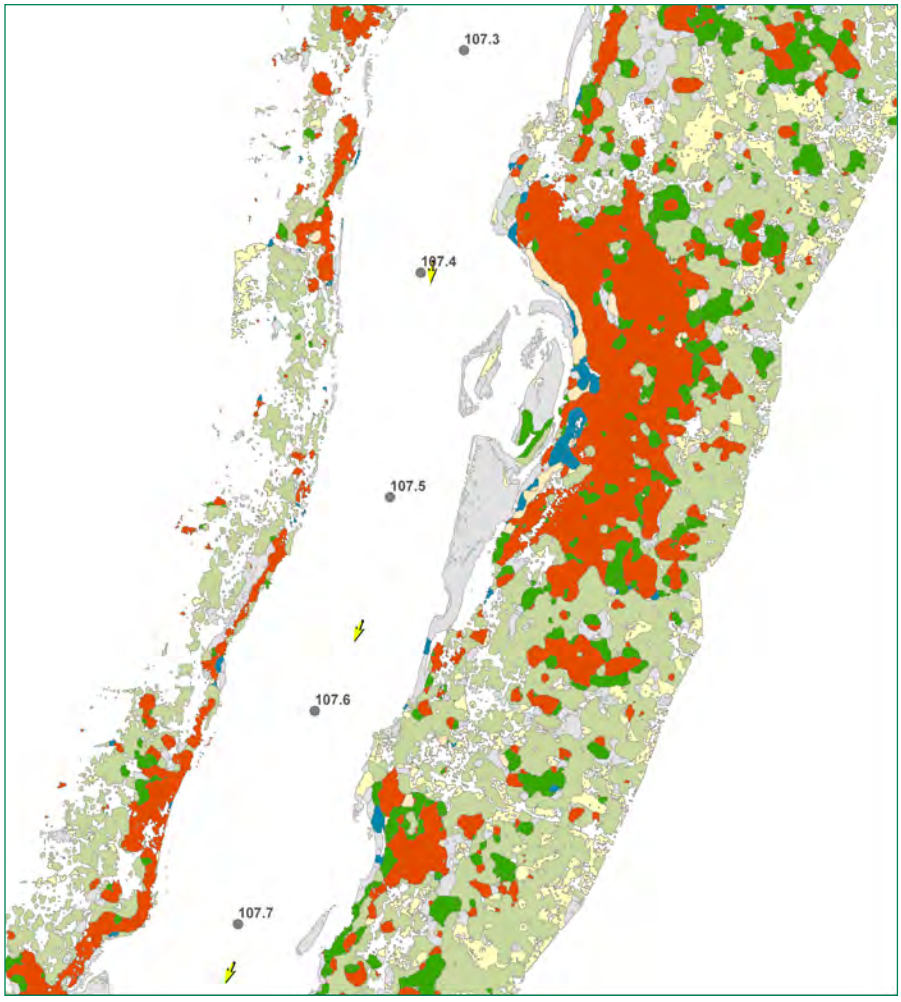

Open-File Report 2008–1216

U.S. Department of the Interior
U.S. Geological Survey

This page intentionally left blank

A Vegetation Database for the Colorado River Ecosystem from Glen Canyon Dam to the Western Boundary of Grand Canyon National Park, Arizona

By Barbara E. Ralston, Philip A. Davis, Robert M. Weber, and Jill M. Rundall

In cooperation with Pinnacle Mapping Technologies, Inc. and Northern Arizona University

Open-File Report 2008–1216

U.S. Department of the Interior
U.S. Geological Survey

U.S. Department of the Interior
DIRK KEMPTHORNE, Secretary

U.S. Geological Survey
Mark D. Myers, Director

U.S. Geological Survey, Reston, Virginia: 2008

For product and ordering information:
World Wide Web: http://www.usgs.gov/pubprod
Telephone: 1-888-ASK-USGS

For more information on the USGS--the Federal source for science about the Earth, its natural and living resources, natural hazards, and the environment:
World Wide Web: http://www.usgs.gov
Telephone: 1-888-ASK-USGS

Suggested citation:
Ralston, Barbara E., Davis, Philip A., Weber, Robert M., and Rundall, Jill M., 2008, A vegetation database for the Colorado River ecosystem from Glen Canyon Dam to the western boundary of Grand Canyon National Park, Arizona: U.S. Geological Survey Open-File Report 2008–1216, 37 p.

Contents

Figures

Tables

A Vegetation Database for the Colorado River Ecosystem from Glen Canyon Dam to the Western Boundary of Grand Canyon National Park, Arizona

By Barbara E. Ralston[1], Philip A. Davis[1], Robert M. Weber[2], and Jill M. Rundall[3]

Executive Summary

A vegetation database of the riparian vegetation located within the Colorado River ecosystem (CRE), a subsection of the Colorado River between Glen Canyon Dam and the western boundary of Grand Canyon National Park, was constructed using four-band image mosaics acquired in May 2002. A digital line scanner was flown over the Colorado River corridor in Arizona by ISTAR Americas, using a Leica ADS–40 digital camera to acquire a digital surface model and four-band image mosaics (blue, green, red, and near-infrared) for vegetation mapping. The primary objective of this mapping project was to develop a digital inventory map of vegetation to enable patch- and landscape-scale change detection, and to establish randomized sampling points for ground surveys of terrestrial fauna (principally, but not exclusively, birds). The vegetation base map was constructed through a combination of ground surveys to identify vegetation classes, image processing, and automated supervised classification procedures. Analysis of the imagery and subsequent supervised classification involved multiple steps to evaluate band quality, band ratios, and vegetation texture and density. Identification of vegetation classes involved collection of cover data throughout the river corridor and subsequent analysis using two-way indicator species analysis (TWINSPAN).

Vegetation was classified into six vegetation classes, following the National Vegetation Classification Standard, based on cover dominance. This analysis indicated that total area covered by all vegetation within the CRE was 3,346 ha. Considering the six vegetation classes, the sparse shrub (SS) class accounted for the greatest amount of vegetation (627 ha) followed by *Pluchea* (PLSE) and *Tamarix* (TARA) at 494 and 366 ha, respectively. The wetland (WTLD) and *Prosopis-Acacia* (PRGL) classes both had similar areal cover values (227 and 213 ha, respectively). *Baccharis-Salix* (BAXX) was the least represented at 94 ha. Accuracy assessment of the supervised classification determined that accuracies varied among vegetation classes from 90% to 49%. Causes for low accuracies were similar spectral signatures among vegetation classes. Fuzzy accuracy assessment improved classification accuracies such that Federal mapping standards of 80% accuracies for all classes were met.

The scale used to quantify vegetation adequately meets the needs of the stakeholder group. Increasing the scale to meet the U.S. Geological Survey (USGS)-National Park Service (NPS) National Mapping Program's minimum mapping unit of 0.5 ha is unwarranted because this scale would reduce the resolution of some classes (e.g., seep willow/coyote willow would likely be combined with tamarisk). While this would undoubtedly improve classification accuracies, it would not provide the community-level information about vegetation change that would benefit stakeholders. The identification of vegetation classes should follow NPS mapping approaches to complement the national effort and should incorporate the alternative analysis for community identification that is being incorporated into newer NPS mapping efforts. National Vegetation Classification is followed in this report for association- to formation-level categories.

Accuracies could be improved by including more environmental variables such as stage elevation in the classification process and incorporating object-based classification methods. Another approach that may address the heterogeneous species issue and classification is to use spectral mixing analysis to estimate the fractional cover of species within each pixel and better quantify the cover of individual species that compose a cover class. Varying flights to capture vegetation at different times of the year might also help separate some vegetation classes, though the cost may be prohibitive. Lastly, photointerpretation instead of automated mapping could be tried. Photointerpretation would likely not improve accuracies in this case, however, because the image quality that was obtained prevented visual differentiation of several major vegetation classes like tamarisk, mesquite, and seep willow. In addition, the time and associated costs necessary to photointerpret the river corridor would be prohibitive.

[1] U.S. Geological Survey, Southwest Biological Science Center, Flagstaff, Ariz.

[2] Pinnacle Mapping Technologies, Inc., Flagstaff, Ariz.

[3] Northern Arizona University, Center for Environmental Science and Education, Flagstaff, Ariz.

The vegetation base map for the CRE provides an initial inventory of the area covered by vegetation and an indication of which species dominate the river corridor. The map is a critical element in assessing the status and trends of riparian vegetation for the CRE at a large scale. It contributes systemwide information that can promote a far-reaching understanding of how dam operations affect biological resources. Beyond helping to assess vegetated area change and vegetation class changes over time, map data can be linked to ecosystem function and structure questions. Specifically, questions can begin to be addressed about how changes in riparian vegetation affect other resources like campsite area, exotic species expansion and control, and food web development in the terrestrial and aquatic system. A long-term systemwide approach to vegetation area inventories, in addition to local-scale measures of change, is a critical tool in monitoring change in riparian vegetation along the river corridor associated with dam operations.

Introduction

Monitoring vegetation at multiple temporal and spatial scales is proving to be the most informative approach for detecting change and inferring causal agents of change (Herbel and others, 1972; Ares and others, 2003; Bestelmeyer and others, 2006). Riparian communities that are tightly linked to annual stream hydrology, ground water elevations, sediment transport, and accompanying disturbance of varying magnitudes over time (Stromberg and others, 1996; Montgomery and MacDonald, 2002; Naiman and others, 2005) are particularly strong candidates for multiscale monitoring. In the arid southwest, where riparian habitats are rare but play an important role in animal sustainability and overall biodiversity (Johnson and others, 1977; Farley and others, 1994), knowing the extent and composition of the riparian community and potential trajectories of change is critical for resource managers.

In 1996, signing of a Record of Decision for the operation of Glen Canyon Dam (Department of the Interior [DOI], 1996) initiated the Glen Canyon Dam Adaptive Management Program and the process of long-term monitoring and assessment of resources affected by dam operations. Previous vegetation research and monitoring in the Colorado River ecosystem (CRE) had focused primarily on local, and to some extent, geomorphic reach-based effects on vegetation relative to dam operations (Anderson and Ruffner, 1987; Stevens, 1989; Waring and Stevens, 1986; Stevens and Ayers, 1993; Stevens and others, 1995; Waring, 1995; Stevens and Ayers, 1997; Kearsley and Ayers, 1999; Howe, 2001; Porter, 2002). Smaller scale evaluations that consider the entire river corridor were limited by the time and cost required for ground surveys. These studies included general plant collections for species lists (Clover and Jotter, 1944; Phillips and others, 1987; Ayers and others, 1994), descriptions of marsh community assemblages relative to dam operations (Stevens and others, 1995), and the operational effects of Glen Canyon Dam on riparian vegetation (Carothers and Aitchison, 1976; Turner and Karpiscak, 1980; Kearsley and Ayers, 1999; Stevens and others, 2001; Ralston, 2005). Work since 1997 has been conducted to support information needs identified by the Glen Canyon Dam Adaptive Management Program.

The only previous quantitative description of vegetation distribution for the length of the river corridor from Glen Canyon Dam to the boundary of Lake Mead was completed by Phillips and others (1977). The map exists only in hard copy, which has limited utility for change detection studies. Since 1977, Glen Canyon Dam operations have included a flood release at 2,747 m^3/s in 1983 (Fradkin, 1984), and reduced peaking operations in association with Record of Decision operation criteria (DOI, 1996). With the initiation of long-term monitoring associated with the Glen Canyon Dam Adaptive Management Program (DOI, 1996), a GIS-based vegetation inventory map was identified as a basic need to conduct long-term, large-scale change detection of vegetation and to increase the statistical rigor associated with ground-based surveys and monitoring (Urquhart and others, 2000). The information needs of the adaptive management program regarding riparian vegetation include quantifying the area change of dominant vegetation classes that occupy areas below and above the postdam high-water zone (approximates 1,416 m^3/s). Changes in riparian vegetation associated with Glen Canyon Dam operations are of the greatest interest.

The primary objective of this mapping project was to develop a digital inventory map of vegetation to enable patch- and landscape-scale change detection, and to establish randomized sampling points for ground surveys of terrestrial fauna (principally, but not exclusively, birds). Digital orthorectified imagery and computer-aided classification provide for larger scale inventory and assessment of riparian resources along the river corridor that complements local or smaller scale monitoring. In 2003, the development of a digital vegetation base map for the CRE was initiated. The advanced state of digital and image-processing technologies suggested that automated classification using digital multiband imagery could be an efficient and feasible option for mapping the corridor's extent. The effort considered the objectives of the mapping project relative to monitoring needs, previous mapping efforts (Phillips and others, 1977; Kearsley and Ayers, 1996), the national vegetation classification standards for the system of National Vegetation Classification (NVC; Grossman and others, 1998), Federal mapping standards (Federal Geographic Data Committee Vegetation Subcommittee, 1997), and the limitations imposed on mapping by the characteristics of the imagery (e.g., spatial resolution, radiometric calibration, and atmospheric corrections). This project utilized two-way indicator species analysis (TWINSPAN; Hill, 1979) to identify major vegetation classes for mapping the river corridor. Image signatures of these classes were used to automate the mapping process, which resulted in a systemwide digital inventory of the riparian vegetation along the river corridor.

Study Area

The riparian zone within the CRE encompasses portions of Glen Canyon Recreational Area, Grand Canyon National Park, and The Hualapai Nation. The corridor from Glen Canyon Dam to the boundary of Lake Mead Recreational Area spans a distance of 474 km and includes pre- and postdam riparian areas approximately 75 m wide along each side of the river corridor, resulting in a total land area of approximately 69,750 km^2. The river channel passes through 13 geomorphic reaches (fig. 1) that vary in width and depth because of differences in the underlying bedrock lithology (Schmidt and Graf, 1990). Within Grand Canyon there are 740 tributaries that produce debris-fan eddy complexes (Schmidt, 1990), which form constrictions and associated rapids along the river. Most tributaries are intermittent rather than permanent sources of water entering the mainstem Colorado River. The debris fans, eddies, and channel margins form the substrate for riparian vegetation. The density and areal coverage of vegetation are influenced by the geographic orientation controlling solar shading and slope aspect (Yard and others, 2005), the type of exposed bedrock, the frequency of debris flows from tributaries that form debris fan-eddy complexes (Schmidt, 1990), flood event variables (e.g., duration, magnitude, and frequency), and other factors (Naiman and Decamps, 1990; Naiman and others, 2005).

The predam riparian zone was subject to annual floods of 1,416 m^3/s, biannual floods of 2,407 m^3/s, and 6-year return floods of up to 3,398 m^3/s (fig. 2; Topping and others, 2003). The largest water volumes through the canyon were associated with spring runoff from watersheds of the Green, Colorado, and San Juan Rivers. Construction of Glen Canyon Dam began in 1956 as a part of the Colorado River Storage Project Act of 1956 (43 United States Code 620) and the dam became operational in 1963. A consequence of water-flow regulation is that the yearly natural disturbance associated with annual runoff was replaced with daily fluctuations associated with dam operations. Summer monsoonal and fall storms still contribute some disturbance to the downstream tributaries in the system. Primary tributaries that contribute to downstream disturbance are the Paria and Little Colorado Rivers, located 15 and 125 km downstream of Glen Canyon Dam, respectively (fig 1).

Besides the loss of a seasonal disturbance pattern, the annual peak discharges along the river were reduced following regulation. Since regulation began in 1963, median annual discharge has varied between 268 and 450 m^3/s. In 1996 (DOI, 1996), operational constraints were placed on Glen Canyon Dam, and the median annual discharge measured at the USGS gage at Lees Ferry (USGS gage number 09380000) through September 2000 was 378 m^3/s (Topping and others, 2003). Glen Canyon Dam is a hydropower dam and discharge fluctuates on a daily basis according to power demand; since 1996, the range of these daily fluctuations has been 138 m^3/s.

The effect of regulation on riparian vegetation was an expansion of vegetation from the predam annual stage elevation shoreward (Carothers and Aitchison, 1976; Turner and Karpiscak, 1980; Waring, 1995; Ralston, 2005). Analysis of selected areas within the corridor that were mapped (Waring, 1995) indicated that vegetated area below the annual flood volume increased by more than 50%. Marsh communities that had limited distribution in Glen Canyon and in Western Grand Canyon prior to regulation expanded throughout the corridor. Today, riparian and marsh vegetation exist throughout the corridor from the shoreline to the predam 6-year return flood stage elevation. The vegetation composition follows a moisture gradient with marsh species and obligate riparian species adjacent to the shoreline and facultative riparian and xerophytic species located upslope. Daily and monthly operations tend to affect vegetation up to the 991-m^3/s stage elevation, while local precipitation affects species composition of areas above and below the 991-m^3/s stage elevation (Kearsley, 2006). Since regulation began, the riparian zone affected by dam operations generally occupies areas below the 1,274-m^3/s stage elevation (Kearsley, 2006; Ralston, 2005), although a spill as high as 2,747 m^3/s did occur in 1983 in association with high spring inflows and resulting high reservoir elevations.

The vegetation composition along the corridor follows a north-south gradient; includes elements from the Great Basin, Mohavean, and Sonoran Desert Scrub Communities (classification per Brown, 1982); and includes exotic species like tamarisk (*Tamarix ramosissima* Ledeb.), camelthorn (A*lhagi maurorum* Medik.), and Bermuda grass (*Cynodon dactylon* [L.] Pers). Prior to regulation, vegetation below the 1416-m^3/s stage elevation (approx. annual return flood) was sparse (Clover and Jotter, 1944) and was composed mostly of seep willow (*Baccharis emoryi* A. Gray), longleaf brickellbush (*Brickelia longifolia* S. Watson), coyote willow (*Salix exigua* Nutt.) and arrowweed (*Pluchea sericea* [Nutt.] Coville), and other herbaceous vegetation. Gooding's willow (*Salix gooddingii* Ball) was present, but sparsely distributed and predominantly associated with flood plain geomorphology like that found at Lees Ferry or in western Grand Canyon.

Vegetation above the 1,416-m^3/s stage elevation included trees and shrubs such as mesquite (*Prosopis glandulosa* Torr.), net leaf hackberry (*Celtis laevigata* Willd. var. *reticulata* [Torr.] L.D. Benson), and tamarisk; small shrubs were also present such as four-wing salt bush (*Atriplex confertifolia* [Torr. and Frém.] S. Watson), brittlebush (*Encelia farinose* A. Gray ex Torr.), and Mormon tea (*Ephedra nevadensis* S. Watson), as well as bunch grasses including sand dropseed (*Sporobolus contractus* Hitchc.), purple three awn (*Aristida purpurea* Nutt.), and old man's beard (*Bothriochloa barbinodes* [Laq.] Herter).

Since the dam became operational, marsh habitat along the CRE has increased (Clover and Jotter, 1944; Turner and Karpiscak, 1980; Stevens and others, 1995) and includes, but is not limited to, common reed (*Phragmites australis* [Cav.] Steud.), cattail (*Typha latifolia* L.), water sedge (*Carex aquatilis* Wahlenb.), rabbitfoot grass (*Polypogon viridis* [Gauan] Breistr.), and Torrey's rush (*Juncus torreyi* Coville) (Phillips and others, 1987).

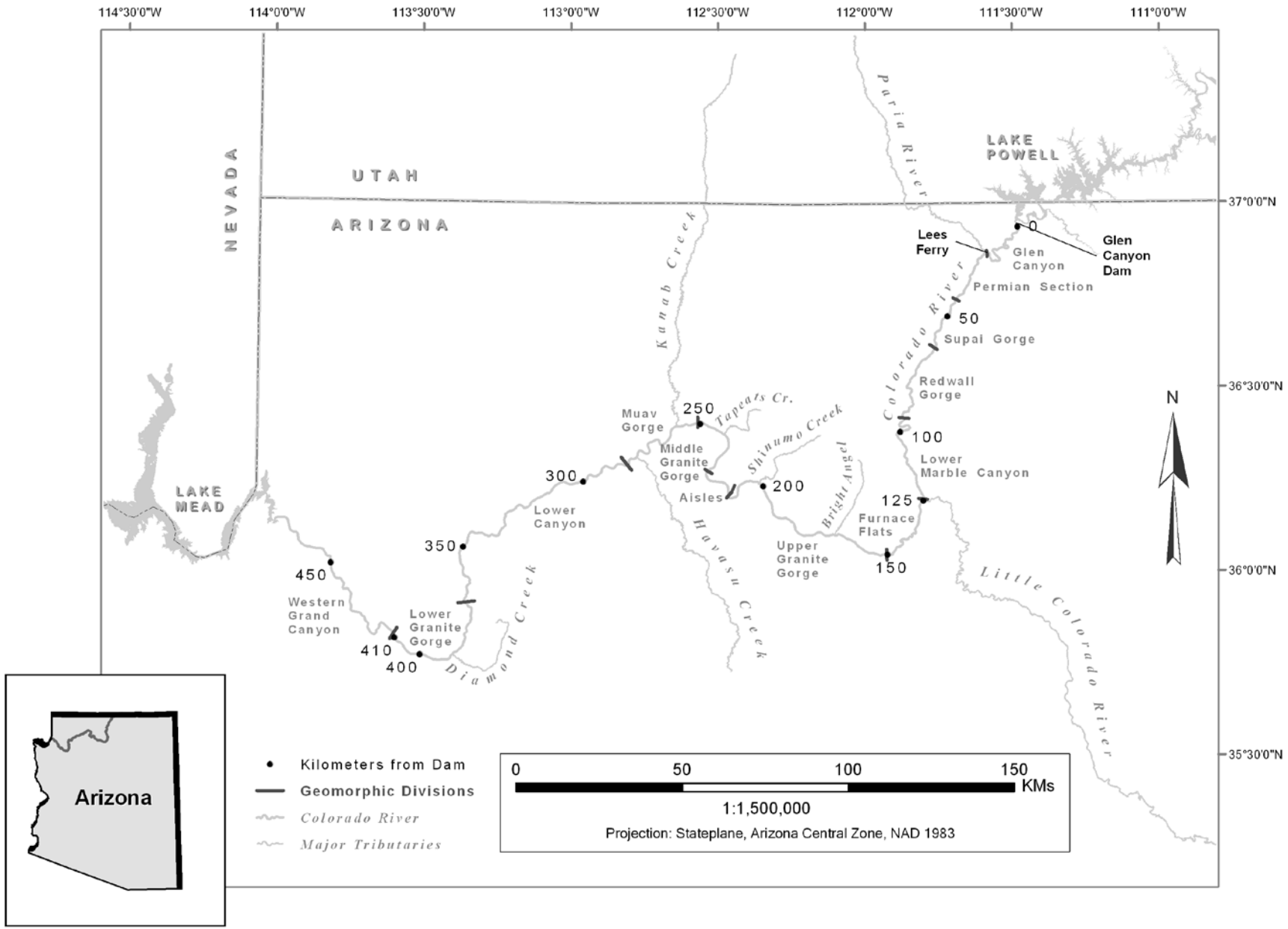

Figure 1. Map of study area from Glen Canyon Dam to Lake Mead with geomorphic reaches indicated by name and distances from the Glen Canyon Dam indicated by kilometer markers or river kilometers.

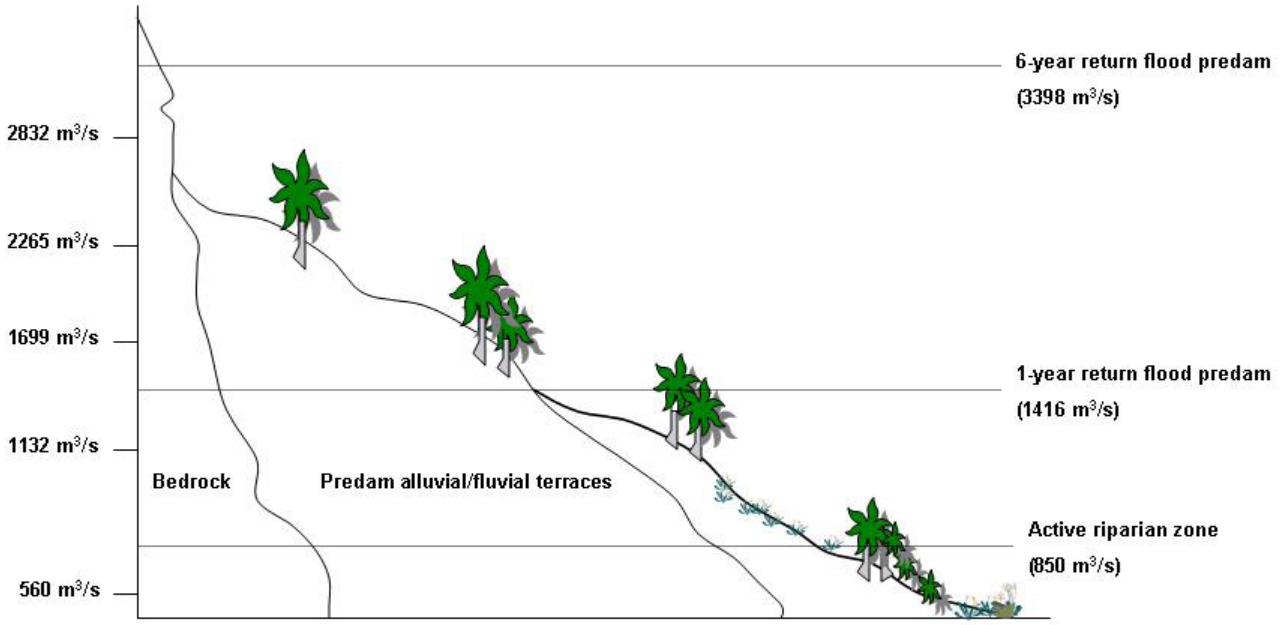

Figure 2. Zonation of vegetation according to river stage. Reduced flood frequencies, determined by releases from Glen Canyon Dam, have resulted in the development of three well-defined vegetation zones: shoreline habitats below the 700-m³/s stage, postdam riparian habitats ("new high-water zone") below the 1460-m³/s stage, and predam riparian habitats ("old high-water zone") above that (Carothers and Aitchison, 1976).

Criteria for Vegetation Class Selection

The first corridorwide vegetation mapping was conducted by Phillips and others (1977) using 13 vegetation types. Vegetation types were categorized following a physiognomic classification scheme and included forest, woodland, scrub, and herbaceous categories, further modified to include leaf type descriptors (e.g., deciduous, evergreen, sclerophyllous, orthophyllous). Their mapping units are comparable to the formation-level units in the NVC. Included in their map key are common species associated with each vegetation type, but an absolute correspondence of vegetation type to dominant species is lacking in this map. Mapped areas included vegetation into the xeric zone (e.g., *Agave*, *Larrea*).

Subsequent mapping efforts did not attempt to cover the river corridor, but focused either on specific sites to document plant community change for relatively small areas (e.g., 50 ha; Kearsley and Ayers, 1996) or on segments of the river corridor (approx. 8 km in length) to map the riparian vegetation at a landscape scale (Waring, 1995). In this latter case, vegetation was classified as either pre- or postdam vegetation and referred to as old or new high-water classes, based on the 1,416-m³/s stage elevation (Waring, 1995). Kearsley and Ayers (1996) used relevé plots to record vegetation cover and species composition in combination with TWINSPAN (Hill, 1979) to delineate community types. Of the two studies, Kearsley and Ayers' (1996) results were more applicable to the mapping objectives described in this report for selecting preliminary vegetation classification units. Though Kearsley and Ayers cautioned that the results of their classification analyses were not applicable to Southwestern regions, their results were useful in formulating the initial vegetation classification units used here because their census included locations throughout the CRE.

This study expands vegetation classification far beyond previous site-specific studies (Stevens and others, 1995; Kearsley and Ayers, 1996) to include riparian shrubs and woodlands along the channel margins and up to the predam 6-year return flood of 3,398-m³/s stage elevation. To monitor community change not only for riparian vegetation but also for faunal constituents, a finer classification scale was used in this study than that used by Phillips and others (1977). The intention was to develop a base map at the alliance or association level following the NVC definition of these categories (Grossman and others, 1998). These levels of classification better represent community assemblages than higher order levels such as the formation level. For questions regarding large-scale vegetation change, such as the change in all vegetation below the new high-water stage, the higher level classification would be appropriate and formation classes could be extracted from the more detailed classes by aggregation. Additionally, because the areal coverage was extensive (474 river kilometers [RK]), the use of unsupervised and supervised classification on recently collected digital imagery was investigated. This report discusses the capabilities of these approaches relative to the objectives and provides summary statistics for all vegetation classes along the CRE.

Methods

Preliminary Vegetation Classes

Preliminary alliance classes were developed from three sources:

1. Previous classification work of Kearsley and Ayers (1996)
2. A combination of existing vegetation classes defined by Natureserve with vegetation classes that were considered to be appropriate for change detection questions identified by adaptive management stakeholders
3. Consideration of remote-sensing and classification capabilities for riparian habitats

Kearsley and Ayers (1996) used cover data from relevé plots and TWINSPAN analysis (Hill, 1979) to characterize nine sites distributed along the river corridor. Their work focused on the communities within these sites, which were at a resolution considered to be appropriate for a base map to monitor riparian habitat.

Kearsley and Ayers (1996) identified four to seven classes per site. Their analysis showed coyote willow co-occurring with tamarisk and seep willow, or, alternatively, any of these species being the single dominant species. Arrowweed was often a monotypic dominate shrub and was designated as a vegetation class. Associated herbaceous vegetation including horsetails (*Equisetum* sp.), water sedge, common reed, and brome grasses (*Bromus* sp.) were also identified as dominant or associated understory species. The Kearsley and Ayers analysis did not include areas above the 1,274-m^3/s stage elevation; additional classes for these higher elevations had to be identified.

The Natureserve Web site (www.natureserve.org) was used to identify alliances that met the species composition of the groups identified by Kearsley and Ayers (1996). Information was also used from Davis and others (2002), who had remapped some of the Kearsley and Ayers sites using a supervised classification to determine which of the Kearsley/Ayers vegetation classes could be adequately separated using digital imagery. In addition, a special status species was included for Grand Canyon National Park (Brian, 2000), satintail (*Imperata brevifolia* Vasey), to determine whether it could be accurately mapped. Nonvegetated classes to address sand and bedrock were added, and it was noted that dried grass and dead brush (i.e., ground litter) produced a widespread signature that needed to be identified. From these sources of information, a preliminary classification was developed of 15 vegetation classes and 3 nonvegetated classes (table 1). Training sites along the corridor that were considered to be representative of these vegetation classes were identified, including those identified by Kearsley and Ayers (1996), for use in the supervised classification process.

Table 1. Preliminary vegetation classes and number of surveyed groundtruth sites containing these classes.

Vegetation class	Species name or description of class	Number of sample sites
ATCA	*Atriplex canescens*	22
BAXX	*Baccharis spp.*	36
CERE	*Celtis reticulata*	32
EQFE	*Equisetum ferrisii*	16
IMBR	*Imperata brevifolia*	29
LATR	*Larrea tridentata*	19
PHAU	*Phragmites australis*	28
PLSE	*Pluchea sericea*	17
PRGL	*Prosopis glandulosa*	28
QUTU	*Quercus turbinella*	34
SAEX	*Salix exigua*	27
SAGO	*Salix goodingii*	39
TARA	*Tamarix ramossisima*	28
TYDO	*Typha domingensis*	36
WTLD	Wetland grasses and sedges	29
BDRX/SAND	Bedrock/sand	10
Dead grass	Litter	4
Dead brush	Litter	17

Verifying Vegetation Classes

To verify the preliminary alliance classes, ground surveys were conducted at randomly generated points along the CRE. The points were generated in ENVI (ITT Visual Information Solutions©, 2006). Relevé plots with a radius of 3 m (approx. 28 m²) were used to record cover dominant species and to compare with the supervised classification results. Plot size was determined by referring to Westhoff and van der Maarel (1978) and was similar to the size used by Kearsley and Ayers (1996). The plot size also corresponded to areal density calculations described in appendix A. For each plot, cover dominant species (following a modified Daubenmire scale, table 2) were recorded, as well as the geomorphic reach of the species, the physiognomic leaf character, and plant heights of dominant plants in the plot. Plant heights were estimated to the nearest 0.5-m increments and recorded. All plants occurring in the plot were listed. In the event that a single or rare species occurred in the plots, the species was noted as a "trace" or "t" on the data sheet and given a value of 0.01 in the spreadsheet.

For most classes, at least 25 plots were surveyed. For rarer vegetation types, at least 10 plots were surveyed. The study began with 578 points; however, some sites were inaccessible or out of the study area. The final database included 451 sample points.

Cover data and associated species were entered into an Access (Microsoft™) database. The vegetation cover data were analyzed using ordination software, PC-ORD v.4 (McCune and Mefford, 1999). TWINSPAN analysis was done for cover values of 3 (25%–50% cover) and 4 (50%–75% cover; table 3*A*, *B*). TWINSPAN was used because it was the standard approach used by the National Mapping Program when this project was initiated. The maximum group size per division, maximum number of indicators, and maximum number of species in the final table were set at 3, 3, and 25, respectively, for all runs.

Table 2. Modified Daubenmire scale for cover values and corresponding percentages of ground cover.

Cover values	Percent of ground cover
Trace	<1%
1	<5%
2	5%–25%
3	25%–50%
4	50%–75%
5	75%–95%
6	>95%

Table 3. Divisions, groups, and corresponding alliance groups identified through TWINSPAN analysis. *A*, Grouping using cover values 3. *B*, Grouping using cover values 4.

A

Group	Alliance
	Division 0
00000	*Phragmites australis*
00001	*Typha domingensis*/*Carex aquatilis*
00001	*Baccharis emoryi*/*Salix exigua*
0001	*Equisetum ferrisii*
001	*Polypogon monspeliensis*
0100	*Baccharis salicifolia*
0101	*Tamarix ramossisima*/*Brickelia longifolia*
011	*Pluchea sericea*/*Aster spinosa*
	Division 1
100	*Bromus rubens*
1010	*Acacia greggi*/*Fallugia paradoxa*
1011	*Prosopis glandulosa*/*Larrea tridentate*/*atriplex canescens*
11	*Baccharis sarothroides*

B

Group	Alliance
	Division 0
00000	*Phragmites*/*Scirpus americanus*
00001	*Typha domingensis*/*Carex aquatilis*
00001	*Baccaharis emoryi*/*Salix exigua*
010	*Tamarisk ramosissima*/*Aster spinosa*
011	*Pluchea sericea*
	Division 1
1	*Prosopis glandulosa*/*Acacia. greggii*/*Baccharis sarothroides*

Digital Data Acquisition

During a 10-day period starting May 30, 2002, a digital line scanner was flown over the Colorado River corridor in Arizona by ISTAR Americas, using a Leica ADS–40 digital camera to acquire a digital surface model and four-band image mosaics (blue, green, red, and near-infrared [NIR]) for vegetation mapping. The timing of the mission was selected to reduce the likelihood of storms, clouds, and shadows; to minimize phase angle changes during image acquisition; and to capture most vegetation with full foliage, although some species leaf out slightly later in the growing season (e.g., common reed and cattails).

Each river reach required multiple, overlapping flight lines; each set of parallel flight lines for a particular river reach was assigned a number or letter designation (fig. 3). The digital surface model (DSM) was derived from three charge-coupled device (CCD) line scanners that recorded ground reflectance within the 520–760-nm wavelength range at a ground resolution of 22 cm. This broadband is referred to as a panchromatic band. The three CCDs looked fore, aft, and nadir along each flight line. Flight lines overlapped by as much as 50%, which provided multiple looks for each ground element along the entire corridor.

Photogrammetric computations applied to these stereo databases produced surface elevation at a 1-m cell spacing with a root-mean-square vertical error of 45 cm. The DSM represents the elevation of visible surface regardless of surface cover, and as such it may be used to derive vegetation heights using nearby bare-ground elevations. The vegetation heights have additional uncertainties due to variable depth of canopy reflection.

Four additional wavelength-band images were collected with the same sensor, using four additional CCD line scanners that collected ground reflectance in the blue (450–510 nm), green (530–576 nm), red (642–682 nm), and NIR (770–814 nm) regions of the electromagnetic spectrum. These data were collected at a ground resolution of 44 cm. The wavelength ranges for the green, red, and NIR bands are close to the suggested ranges for three of the four bands that were judged to be optimum for discriminating vegetation within the CRE (Davis and others, 2002).

Supervised Classification Analyses of the Groundtruth Regions

Following image processing procedures that evaluated band quality, band ratios, and vegetation texture and density (see more detailed information in appendix A), 15 possible databases were identified for use in vegetation classification: four bands, their six-band ratios, four-texture measures, and vegetation density. Different supervised classifiers were run on these data for the various groundtruth regions within the CRE to determine the type of classifier that produced the highest accuracy. For these analyses, all groundtruth areas were mosaicked into a single 15-band image and designated pixels representative of the various vegetation alliances. The types of classifiers tested included parallelepiped, minimum distance, Mahalanobis distance, maximum likelihood, and spectral angle mapper. The maximum likelihood produced the highest mapping accuracies, which was also found by Davis and others (2002). Maximum likelihood classifications were then performed on each groundtruth region using different combinations of the 15 possible databases. Analyses of image classification results indicated that the combination of the four-band data and four-texture measures most accurately reproduced the groundtruth vegetation maps, and this combination was used in the final vegetation classification processing (see more detailed information in appendix A).

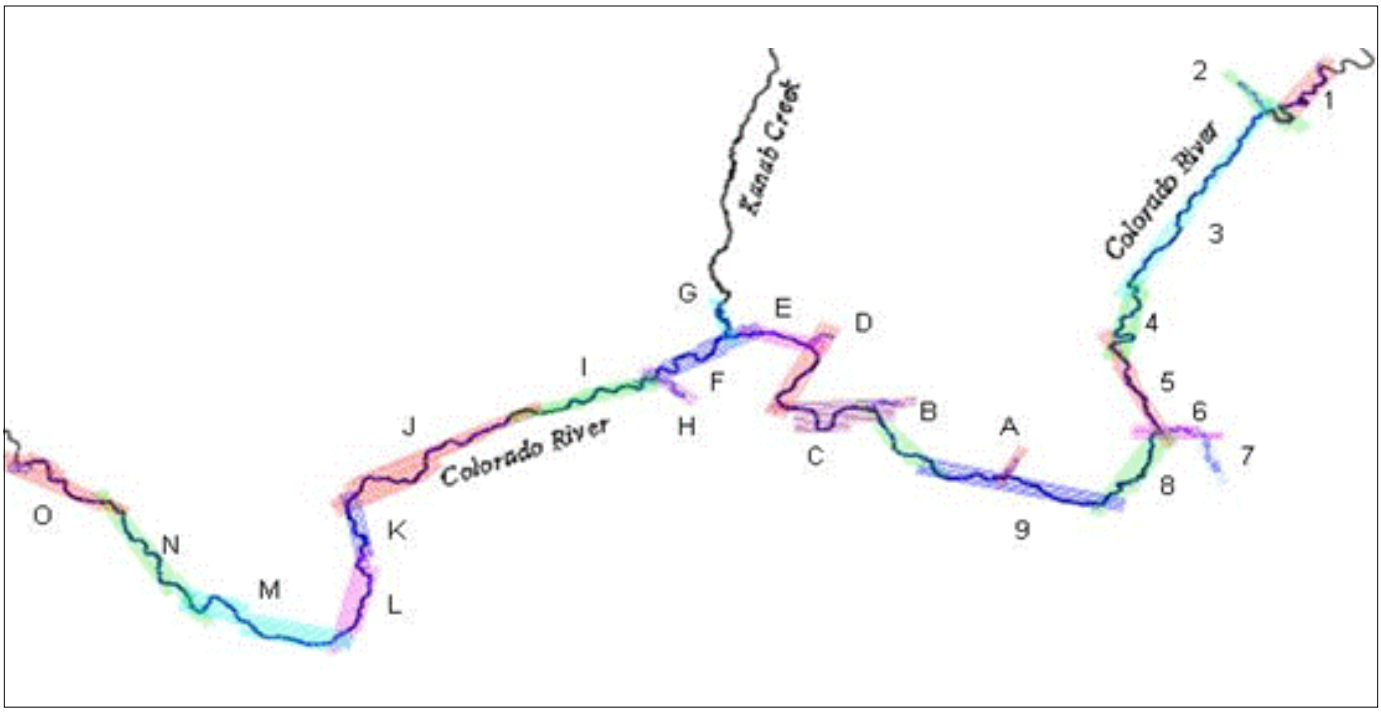

Figure 3. Index map of flight lines used in ISTAR airborne data collection in late May–early June 2002. Sets of lines with the same color represent repetitive data collections with 50% overlap; each set of flight lines is labeled with a number or letter.

Accuracy Assessment of Vegetation Classification

Confusion matrices (Congalton, 1991) were constructed for the identified vegetation and unvegetated classes to determine classification accuracies. For these assessments, groundtruth vegetation polygons were compared with supervised classification polygons with areas greater than 0.01 ha. Groundtruth vegetation polygons were delineated in October 2003 and June 2004 with a minimum mapping scale of 0.01 ha. Groundtruth polygons were designated using the identified mapping classes.

Fuzzy Accuracy Assessment

Comparing accuracies between pixel-based classified imagery and groundtruth polygons presented scale problems. Fuzzy accuracy assessment was also employed to assess map classification accuracies. Fuzzy accuracy assessment was first described by Gopal and Woodcock (1994) as an alternative assessment approach that allows for degrees of membership to particular classes. Accuracies are assessed in categories of agreement rather than in a binary assessment such that a class might be "mostly correct" instead of simply "correct" or "incorrect." Three criteria were used in the fuzzy sets, including the strictly "correct" value associated with binary assessment. These criteria have been used by the USGS-NPS National Vegetation Mapping Program (Klopfer and others, 2002; Hansen and others, 2004; Salas, unpub. data). The three criteria are as follows: criterion 5 (exact match), when the groundtruth and pixel-based map-class data match exactly; criterion 4 (acceptable error), when the majority (>50%) of the pixel-based map class match the groundtruth polygon; and criterion 3 (understandable error), when the pixel-based map signature of the vegetation may be similar, possibly due to the density of the dominant vegetation, but was misidentified. If adjacent map classes permitted the likely identification of the map class to the exclusion of the assigned map class, this was also taken into consideration (for example *Prosopis* classified as *Tamarix*, but the plant is too high in elevation to be *Tamarix*).

Mapping Scale

The groundtruth for this study was mapped at .01 ha based on habitat surveys for birds and ground transects for small mammals (Kearsley and others, 2006). The minimum mapping unit for this map was smaller than the conventional mapping unit used in the USGS-NPS National Mapping Program, which is 0.5 ha (The Nature Conservancy, 1994). Filters used in the supervised classification of the imagery ranged in size from 4 to 10 m (appendix A). Mapping at the scale used in the National Mapping Program for the national parks would have resulted in a dilution of community change information that the Glen Canyon Dam Adaptive Management Program identified in their information needs for riparian vegetation. Vegetation information for a larger minimum mapping unit can be obtained by using formation-level categories; by combining alliances, such as tamarisk and seep willow classes, within an ArcMap™ (ESRI©, ArcMap 9.2) framework; or by reanalyzing the imagery at a coarser scale.

Results

Revision of Alliance-Level Classification

TWINSPAN analysis revealed 12 and 6 interpretable vegetation classes for cover values 3 and 4, respectively (table 3*A* and *B*). The first division separated higher elevation xeromorphic and facultative riparian vegetation from lower elevation facultative and obligate riparian and marsh vegetation. Within group "0," species fell out along a hydrologic gradient that separated obligate wetland and riparian species from facultative species. The greatest difference in groups between cover values 3 and 4 is the identification of more herbaceous groups in division 1 for cover value 3. These herbaceous groups tend to grow in monotypic patches, such as red brome (*Bromus rubens* L.), common reed, or annual rabbit's foot grass (*Polypogon monospeliensis* [L.] Desf).

The identified classes also varied slightly from the initial classification that was used here. The greatest disagreements between the TWINSPAN results and the initial classification are differentiation among *Baccharis* species and the absence of a separate *Salix exigua* class (it is combined with *Baccharis emoryi*) in the TWINSPAN results. For cover value 3, *Baccharis emoryi* and *B. salicifolia* (Ruiz and Pav.) Pers. are separate classes. *Baccharis salicifolia* becomes a subordinate species for cover value 4. The initial classification in this study lumped both of these species into a general category of *Baccharis* (BAXX) and thus agreed with the TWINSPAN analysis for cover value 4. Catclaw acacia (*Acacia greggii* A. Gray) and mesquite were also separated in cover value 3, but these species co-occur in cover value 4. Catclaw acacia was not initially identified as a separate class.

Based on the TWINSPAN results for cover value 4 and the accuracies obtained from the supervised classification results, classes that had similar signatures and corresponded to the results of the TWINSPAN group analyses (table 1) were aggregated. The limitations of the imagery also required aggregating wetland species groups into a single class called "wetland." "Seasonal dry grass" was collapsed into the wetland class because this signature at times represented common reed or other nearshore herbaceous species like Bermuda grass. A sparse shrub (SS) class was also included composed of perennial grasses and forbs with small leaf areas, similar reflectance values, and low ground cover percentages (<25%; cover values of 1 or 2), like four-wing saltbush and creosote bush (*Larrea tridentata* [DC.] Coville), Mormon tea, and

brittlebush. Lastly, litter, sand, and rock were combined into a single "nonvegetated" class. The resulting seven classes and corresponding National Vegetation Classification (NVC) categories for vegetation are listed in table 4. Subsequent accuracy assessments were performed on these seven classes using groundtruth data collected in October 2003 and June 2004. The attribute table appearing in the digital vegetation map includes the preliminary vegetation classes (table 1), the aggregated vegetation classes, and the corresponding NVC alliance and formation classes (table 4).

Revised Vegetation Classes and Related National Vegetation Classification Alliances

The six revised vegetation classes (with abbreviations) and their corresponding NVC alliance names that were used in the final vegetation map are described below. The nonvegetation class is also described with less detail.

1. Wetland (WTLD)—*Phragmites australis*/*Scirpus americanus* combined with *Typha latifolia*/*Carex aquatilis*—A patchily distributed assemblage that occurs throughout the river corridor. It is usually found at ca. 266 m³/s (base flow) through the 566 m³/s stage elevation. Substrate is silt to fine sand associated with low-velocity channel margin habitats (e.g., return channels) along rocky and vegetated shorelines, rarely associated with talus slopes. *Typha*, *Carex*, or *Phragmites* often dominate with cover ranging from 50% to 90% of the area. Associated species are sparsely interspersed or along the edges of the community. This class can be obscured in imagery by overhanging shrubs like *Tamarix* or *Baccharis*. Vegetation heights vary from prostrate herbs to *Phragmites* and *Typha* reaching heights of 2 m. Associated species include *Polypogon monosplenis*, *Veronica americana*, *Conyza canadensis*, *Euthamea occidentalis*, *Gnaphalium chinensis*, *Agrostis semiverticilate*, *Cynodon dactylon*, *Elymus canadensis*, *Muhlenbergia asperifolia*, *Juncus balticus*, and *J. torreyii*.

Wetland (WTLD)	
NVC Formation Class	Herbaceous Vegetation
NVC Formation Name	Semipermanently Flooded Temperate or Subpolar Grassland
NVC Alliance	Typha (*angustifolia, latifolia*)—(*Schoenoplectus* spp.) Semipermanently Flooded Herbaceous Alliance
NVC Association	*Typha* (*angustifolia, domingensis*, *latifolia*)—(*Schoenoplectus americanus*) Herbaceous Vegetation

2. *Baccharis emoryi*/*Salix exigua* (BAXX)—A very heterogeneous community found throughout the river corridor in sparse to dense patches. Both dominant species can be found singly, or they can codominate and intermingle with tamarisk. *Baccharis emoryi* often forms dense thick patches with canopy cover values up to 75% interspersed with *Salix exigua*. The shrubs reach heights of 2–3 m. The associated understory is often sparse with ground cover <10%. The community is found close to the shoreline at stage elevations between approximately 566 and 877 m³/s. It is found along channel margins and the downriver side of debris fans and can be overhanging the wetland community. The substrate varies from fine to coarse sand occasionally interspersed with cobbles and boulders. Rarely associated with talus slopes or, if so, then cover is minimal. Associated species include shrubs such as *Salix goodingii* (rare), *Baccharis salicifolia*, and *Brickellia longifolia*, and herbs such as *Equisetum ferrisii*, *Conyza canadensis*, and *Alhaghi maurorum*.

Baccharis emoryi/*Salix exigua* (BAXX)	
NVC Formation Class	Shrubland
NVC Formation Name	Seasonally Flooded Cold-Deciduous Shrubland
NVC Alliance	*Baccharis emoryi* Seasonally Flooded Shrubland Alliance
NVC Association	*Baccharis emoryi-Salix exigua* Shrubland

3. *Tamarix ramosissima*/*Aster spinosa* (TARA)—A ubiquitous community found throughout the CRE that can be variable with respect to the density and age of stands. Older individuals within stands can be very tall (up to 7 m) and have a dense canopy of over 75% with little understory, while younger individuals in newer stands may be more dispersed with cover varying from 25% to 50% and interspersed with annual grasses and forbs and other shrubs like *Baccharis* or *Pluchea*. Found in dense patches along channel margins and in more dispersed stands or patches on debris fans and in talus slopes from 226 m³/s (base flow) to 1,274 m³/s. Substrate is mostly sandy though individuals can be found interspersed in cobbles. Associated species include shrubs such as *Prosopis glandulosa*, *Pluchea sericea*, *Baccharis emoryi*, *Brickellia longifolia*, and *Salix exigua*, and herbs such as *Lepidium latifolia*, *Bromus rubens*, *Bromus tectorum*, *Cynodon dactylon*, and *Equisetum ferrisii*.

Tamarix ramosissima/*Aster spinosa* (TARA)	
NVC Formation Class	Shrubland
NVC Formation Name	Temporarily Flooded Microphyllous Shrubland
NVC Alliance	*Tamarix* spp. Seminatural Temporarily Flooded Shrubland Alliance
NVC Association	*Tamarix* spp. Temporarily Flooded Shrubland

4. *Pluchea sericea* (PLSE)—A homogeneous community in which cover varies from 25% to 75%. When cover is low, the signature for this community is easily confused with sparse shrub. Plants can grow to 1.5 m tall with sparse understory or associated species. Found along chan-

Table 4. Revised vegetation classes for the Colorado River ecosystem.

Group analysis	NVC association	NVC alliance	Unique identifier	Formation name	Formation class
Phragmites/*Scirpus*, combined with *Typha domingensis*/*Carex aquatilis* (WTLD)	*Typha* (*angustifolia, domingensis*, *latifolia*)—(*Schoenoplectus americanus*) Herbaceous Vegetation	*Typha* (*angustifolia*, *latifolia*)—(*Schoenoplectus spp*.) Semipermanently Flooded Herbaceous Alliance	CEGL002010	V.A.5.N.I—Semipermanently Flooded Temperate or Subpolar Grassland	V—Herbaceous Vegetation
Baccharis emoryi/*Salix exigua* (BAXX)	*Baccharis emoryi-Salix exigua* Shrubland	*Baccharis emoryi* Seasonally Flooded Shrubland Alliance	CEGL005947	III.B.2.N.e—Seasonally Flooded Cold-Deciduous Shrubland	III—Shrubland
Tamarix ramosissima/*Aster spinosa* (TARA)	*Tamarix ramosissima* Semi-natural Temporarily Flooded Shrubland	*Tamarix ramossisima* Semi-natural Flooded Shrubland Alliance	CEGL003114	III.A.4.N.c—Temporarily Flooded Microphyllous Shrubland	III—Shrubland
Pluchea sericea (PLSE)	*Pluchea sericea* Seasonally Flooded Shrubland	*Pluchea sericea* Seasonally Flooded Shrubland Alliance	CEGL003080	III.A.2.N.h—Seasonally Flooded Shrubland	III—Shrubland
Prosopis glandulosa/*Acacia greggii*/*Baccharis sarothroides* (PRGL)	*Prosopis glandulosa-Acacia greggii* Temporarily Flooded Woodland	*Prosopis glandulosa* Temporarily Flooded Woodland	CEGL004934	II.B.2.N.b—Temporarily Flooded Cold-Deciduous Woodland	II—Woodland
Sparse shrub (SS)	*Encelia farinosa-Ephedra nevadensis-Ephedra viridis* Shrubland or *Gutierrezia sarothrae* Dwarf Shrubland	*Encelia farinosa* Shrubland Alliance or *Gutierrezia* Dwarf Shrubland	CEGL001252 or A2528	III. A.5.N.b—Facultatively Deciduous Extremely Xeromorphic Subdesert Shrubland or Caespitose Cold-Deciduous Dwarf Shrubland	III—Shrubland or IV—Dwarf Shrubland
Nonvegetated (NV)					

nel margins occupying habitat upslope of tamarisk and seep willow. Associated with stage elevations between 708 and 1,274 m³/s in sand or alluvial gravel substrates. Often encroaches on campsites. Associated species: *Aster spinosa* and *Bromus tectorum*.

Pluchea sericea (PLSE)	
NVC Formation Class	Shrubland
NVC Formation Name	Seasonally Flooded Shrubland
NVC Alliance	*Pluchea sericea* Seasonally Flooded Shrubland Alliance
NVC Association	*Pluchea sericea* Seasonally Flooded Shrubland [Placeholder]

5. *Prosopis glandulosa*/*Acacia greggii* (PRGL)—A sparsely vegetated and variable community assemblage with canopy cover often <50%. Dominant species represent the relictual predam riparian community. Substrate is fine-grained alluvial terraces associated with predam fluvial deposits with gravels interspersed. Often growing on slopes and at stage elevations above 1,274 m³/s. Dominant species occur singly or form codominant patches. Trees grow to 5 m tall with wide canopies. Understory species cover is low. Individuals of these species, particularly *Prosopis*, can also be found associated with tamarisk closer to the river channel. Associated species: *Atriplex canescens*, *Ephedra nevadensis*, *Fallugia paradoxa*, *Lepidium montana*, and *Bromus tectorum*.

Prosopis glandulosa/*Acacia greggii* (PRGL)	
NVC Formation Class	Woodland
NVC Formation Name	Temporarily Flooded Cold-Deciduous Woodland
NVC Alliance	*Prosopis glandulosa* Temporarily Flooded Woodland
NVC Association	*Prosopis glandulosa-Acacia greggii* Temporarily Flooded Woodland

6. Sparse shrub (SS)—A variable community dispersed throughout the CRE composed of low-density perennial herbs and bunch grasses and occurring across all stage elevations above 566 m³/s. Ground cover is <25%, and plants vary in height from <.5 to 1 m tall. Substrate is variable and includes fine alluvial predam flood deposits, desert gravel, debris fans, talus slopes, and shoreline sand deposits. Primarily represented by dwarf shrub species (e.g., *Gutierrezia sarothrae*) and xeromorphic forbs (e.g., *Encelia farinosa*, *Opuntia* spp.), though it can include single tamarisk or willow seedlings found along the shoreline. Associated species: *Ephedra viridis*, *E. nevadensis*, *Acacia greggii*, *Eriogonum inflatum*, *Sporobolus airiodes*, *Aristida purpurea*, *Hesperostipa comata*, and *Bromus tectorum*.

Sparse shrub (SS)	
NVC Formation Class	Bland or Dwarf Shrubland
NVC Formation Name	Facultatively Deciduous Extremely Xeromorphic Subdesert Shrubland or Caespitose Cold-Deciduous Dwarf Shrubland
NVC Alliance	*Encelia farinosa* Shrubland Alliance or *Gutierrezia* Dwarf Shrubland Alliance
NVC Association	*Encelia farinosa—Ephedra nevadensis—Ephedra viridis* Shrubland or *Gutierrezia sarothrae* Dwarf Shrubland

7. Nonvegetated (NV)—Open areas occurring throughout the CRE. Generally absent of live vegetation, or if vegetation is present, it is of such low density that image analysis could not separate vegetation from sand, rocks, or litter. Substrate varies from silt, sand, and gravels to boulders on debris fans, talus slopes, and shorelines.

Vegetation Classification Accuracies

Class accuracies for the seven classes based on criterion 5 were quite variable, with an overall accuracy of 49.2% (table 5*A*). Two classes, SS and mesquite/acacia (PRGL), had ≥80% user and producer accuracies, respectively. Accuracies improved with fuzzy set criteria applied to the standard dataset. Criterion 4 produced much higher accuracies (≥50%) for all classes (tables 5*B*, 6); BAXX, TARA, PRGL, and WTLD classes were assigned "acceptable error" with user accuracies >80%, and SS, PLSE, and WTLD have producer accuracies ≥80% (tables 5*B*, 6). Overall accuracy for the seven classes under criterion 4 increased to 79.5%. Criterion 3 resulted in all classes with ≥80% producer and user accuracies (tables 5*C*, 6). Overall accuracy for the seven classes under criterion 3 increased to 95%.

Electronic Map Organization

The groundtruth vegetation surveys and the vectorized classification maps are in the GCVEG_2006 database that was created using ArcMap. The database has Federal Geographic Data Committee compliant metadata. The database is divided into three personal geodatabases (Microsoft Access files with spatial information created by ESRI with the release of ArcGIS) due to the amount of data: segment I, RK 0–124; segment II, RK 124–267; and segment III, RK 267–474. Each geodatabase has the groundtruth data and associated zones that correspond with the flight lines of the 2002 imagery (fig. 3). An example of the vegetation map and attribute table is provided in figure 4. The map is posted on the Grand Canyon Monitoring and Research Center (GCMRC) Internet map server: http://www.gcmrc.gov/website/vegmap2002/Run.htm.

Table 5. Accuracy assessment of revised vegetation classes reflecting accuracies using fuzzy logic. *A*, criterion 5 (exact agreement). *B*, criterion 4 (acceptable). *C*, criterion 3 (understandable). BAXX = Baccharis emoryi/Salix exigua, PRGL = Prosopis glandulosa/Acacia greggii/Baccharis sarothroides, TARA = *Tamarix ramosissima*/*Aster spinosa*, PLSE = *Pluchea sericea*, SS = sparse shrub, and WTLD = *Phragmites*/*Scirpus*, combined with *Typha domingensis*/*Carex aquatilis*.

A

Vegetation class	BAXX	PRGL	TARA	PLSE	SS	WTLD	Total	User's accuracy
BAXX	5	0	5	7	0	7	24	0.208
PRGL	1	20	9	9	6	6	51	0.392
TARA	2	2	18	8	0	1	31	0.581
PLSE	0	3	0	17	0	7	27	0.629
SS	0	0	0	3	14	0	17	0.824
WTLD	3	0	2	3	12	19	39	0.487
Total	11	25	34	47	32	40	189	
				Accuracy				
Producer's accuracy	0.454	0.800	0.529	0.362	0.438	0.475		93
Overall accuracy								0.492

B

Vegetation class	BAXX	SS	PRGL	TARA	PLSE	WTLD	Total	User's accuracy
BAXX	12	0	0	4	3	5	24	0.500
SS	0	17	0	0	0	0	17	1.000
PRGL	0	4	34	2	3	0	43	0.791
TARA	1	0	0	24	6	0	31	0.774
PLSE	0	2	0	0	25	0	27	0.926
WTLD	0	4	0	0	3	32	39	0.820
Total	13	27	34	30	40	37	181	
				Accuracy				
Producer's accuracy	0.923	0.630	1.000	0.800	0.625	0.865		144
Overall accuracy								0.796

C

Vegetation class	BAXX	SS	PRGL	TARA	PLSE	WTLD	Total	User's accuracy
BAXX	21	0	0	1	2	0	24	0.875
SS	0	17	0	0	0	0	17	1.000
PRGL	0	0	41	0	2	0	43	0.954
TARA	0	0	0	31	0	0	31	1.000
PLSE	0	0	0	0	27	0	27	1.000
WTLD	0	4	0	0	0	37	41	0.902
Total	21	21	41	32	31	37	183	
				Accuracy				
Producer's accuracy	1.000	0.809	1.000	0.969	0.871	1.000		174
Overall accuracy								0.951

Table 6. Percent commission and omission, rank of accuracy, and explanation of the classification results for the aggregated vegetation classes.

Colorado River ecosystem vegetation class	Percent comission	Percent omission	Explanation for error
Phragmites/*Scirpus*, combined with *Typha domingensis*/*Carex aquatilis* (WTLD)	82.0% acceptable	86.4% acceptable	Confused with sparse shrub when vegetation is in low density. Overstory of *Baccharis* and tamarisk may obscure signature.
Baccharis emoryi/*Salix exigua* (BAXX)	87.5% understandable	92.3% acceptable	Confused with *Pluchea* and tamarisk when in sparse form. Can intergress with tamarisk and be codominant.
Tamarix ramosissima/*Aster spinosa* (TARA)	100% understandable	80% acceptable	Most often confused with *Pluchea*, particularly when tamarisk is in low density. Ground reflectance signature influences misclassification.
Pluchea sericea (PLSE)	92.5% acceptable	87.1% understandable	Most often confused with sparse shrub class. Density gradient in combination with stage elevation information may help identification of this species.
Prosopis glandulosa/*Acacia greggii*/*Baccharis sarothroides* (PRGL)	80% exact	100% acceptable	Confused most often with tamarisk due to similar color signature and occasional canopy architecture. Can also be confused with *Pluchea* if in low density. Stage elevation information can be used to help discriminate this class.
Sparse shrub (SS)	80.9% understandable	82.3% exact	Most often confused with *Pluchea*. Density gradient for this class difficult to define.

Summary of Vegetation Cover Within the Colorado River Ecosystem in 2002

The total area covered by all vegetation within the CRE was 3,346 ha (table 7). Considering the six vegetation classes (table 7, figs. 5*A*, *B*), the SS class accounts for the greatest amount of vegetation (627 ha) followed by PLSE and TARA at 495 and 367 ha, respectively. WTLD and PRGL had similar areal cover values (227 and 213 ha, respectively). BAXX is least represented at 94 ha. When the vegetated area is compared between reaches (figs. 6, 7*A–F*), a general trend of increasing vegetated area with distance from the dam is observed.

Vegetation Distribution and Areal Cover Patterns

The lower Marble Canyon, Lower Canyon, and western Grand Canyon reaches (table 7, figs. 1, 6, 7*A–F*) show the greatest area cover for each vegetation class. The SS category has the greatest areal cover (figs. 5*A*, *B*) and could include single tamarisk and willow saplings as well as other species. The SS category gives an indication of the patchy nature of vegetation within the corridor. The data also indicate that Pluchea covers a larger area than *Tamarix* (fig. 7*C*, *D*). Wetlands cover only 7% less area than tamarisk, though tamarisk individuals are also likely to be included as part of the SS category. Thus, area for *Tamarix* may be greater than is represented by the classified values.

Discussion

Vegetation Classification and Remote-Sensing Accuracies

Vegetation along the CRE can be categorized into six classes that represent single or codominant species. The vegetation classes identified in this mapping effort agreed with existing associations and alliances that were defined by the NVC and are available on the Natureserve Web site. Alternative methods of identifying vegetation classes could include hierarchical agglomerative cluster analysis, nonmetric multidimensional scaling, and indicator species analysis, which is being used by the USGS-NPS mapping program (Vanderhorst and others, 2007). The TWINSPAN method, which was previously used in the National Mapping Program, has been subject to criticism in recent years (McCune and Grace, 2002). Subsequent mapping efforts will employ the alternative approaches described above. Changes in classification of CRE vegetation related to the use of these alternative approaches instead of the TWINSPAN method are unlikely. The problems with TWINSPAN classifications have been associated with the grouping of rare species (McCune and Grace, 2002), whereas the six vegetation classes presented here are for dominant cover species.

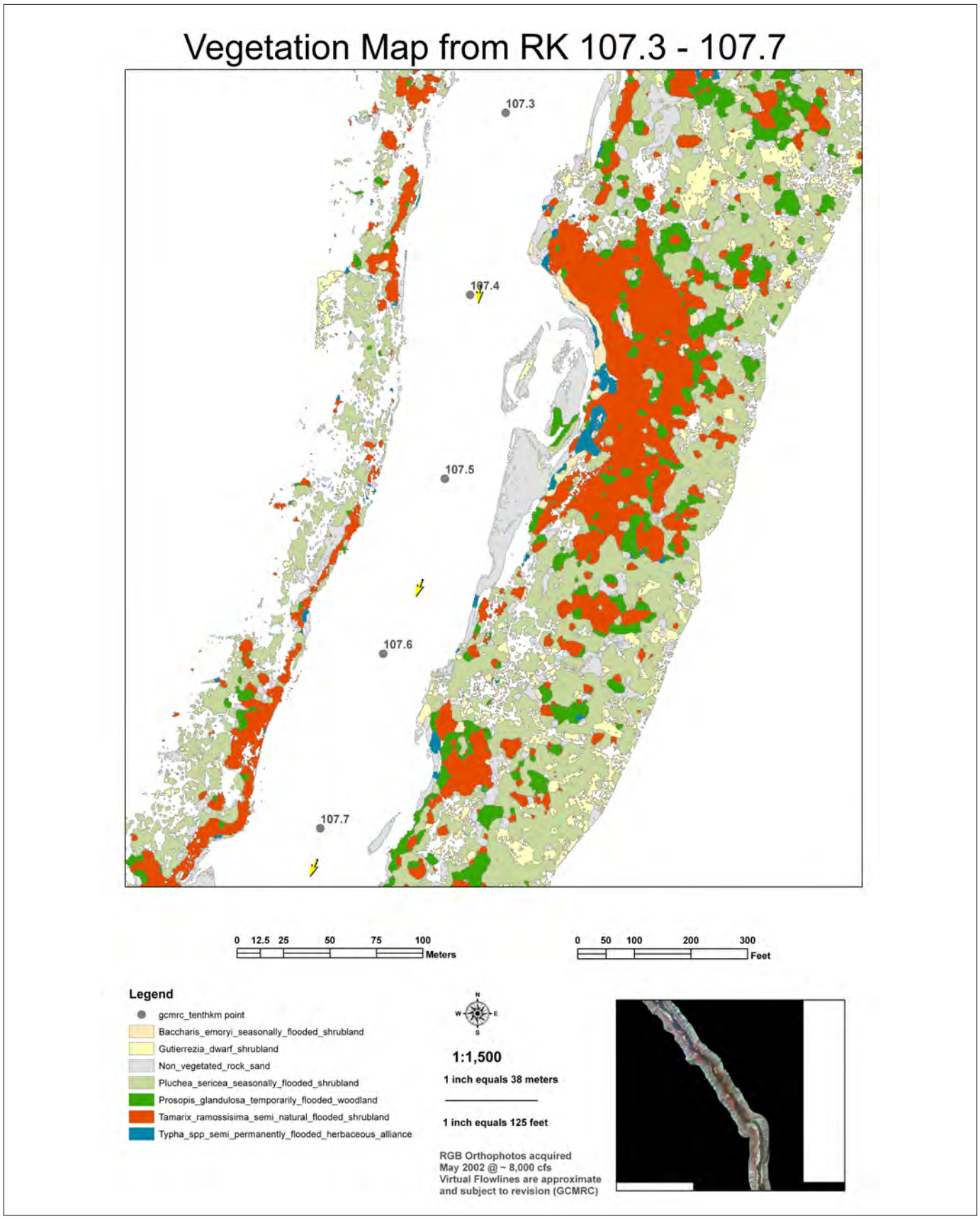

Figure 4. Example of vegetation map from RK 107.3–107.7 with National Vegetation Classification Alliance classes color coded in the legend.

Table 7. Area (in hectares) of mapped classes, of total vegetation mapped, and of total land mass within each geomorphic reach.

Vegetation Class	Glen Canyon	Permian	Supai Gorge	Redwall	Lower Marble	Furnace Flats	Upper Granite	Aisles	Middle Granite	Muav Gorge	Lower Canyon	Lower Granite Gorge	Western Grand Canyon
PRGL/ACGR	7.48	0.18	0.00	0.20	16.16	30.32	1.54	1.23	1.09	0.52	33.98	3.07	117.37
SS	52.25	9.36	0.13	13.10	63.87	21.12	59.82	20.89	21.00	32.43	172.24	40.39	120.41
BAXX/SAEX	3.02	0.79	3.26	0.40	8.72	1.69	1.80	0.91	0.90	0.75	12.28	3.12	56.88
TARA	21.83	10.00	10.94	4.24	37.39	9.16	11.94	2.89	2.56	2.40	50.98	8.16	194.50
PLSE	30.81	24.11	0.00	9.98	88.32	31.93	56.36	12.60	12.11	17.65	82.23	16.96	111.42
NV	49.90	10.29	12.59	26.75	82.34	20.99	113.36	33.37	33.69	22.12	94.64	40.90	46.41
WTLD	17.71	2.18	2.62	3.60	17.75	10.50	16.78	8.16	5.40	4.45	28.31	9.79	100.10
Area													
Total area mapped (ha)	183.00	56.92	29.54	58.27	314.56	125.71	261.59	80.05	76.76	80.32	474.66	122.38	747.08
Total vegetated area (ha)	133.10	46.62	16.95	31.52	232.22	104.72	148.24	46.68	43.07	58.21	380.02	81.48	700.68
Percent vegetated area	73	82	56	55	74	83	56	59	56	72	80	66	93

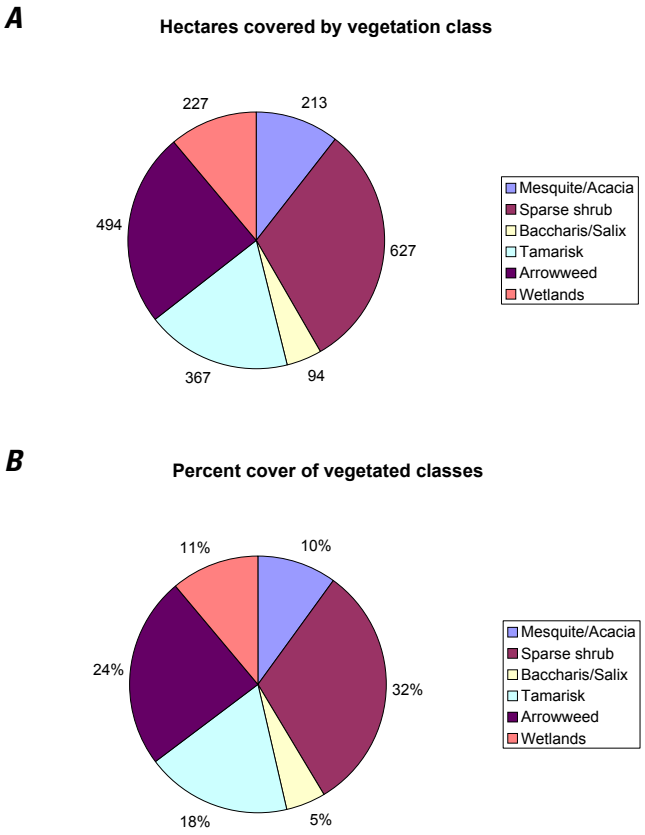

Figure 5. Vegetation map classes. *A*, Percent areal cover of each class for the Colorado River ecosystem (CRE). *B*, Total area of each class for the CRE.

Image Quality

The combination of vegetation density, variable color band reflectance values within and among species, and saturation of the NIR color band often caused signatures to be misclassified in all classes. The reflectance values for *Tamarix* varied widely depending on its density and location along the river, and its signature was confused with most other classes (table 5*A*; appendix A, tables A2–A5). Similarly, the ability to differentiate between types of wetland species (e.g., *Phragmites* vs. *Typha*) was hampered by similar signatures among all wetland species. Others (Ehleringer, 1981; Mooney and others, 1977) have determined that spectral similarity among arid species can occur for multiple reasons, including reduced leaf absorption in the visible range by arid-adapted species; individual response of plants to small precipitation events, which affect spectral variability among individuals of single species (Duncan and others, 1993); and different canopy structures within a species, which affect reflectance (Huete and Jackson, 1988; Hurcom and Harisson, 1998). All of these variables likely affected the spectral patterns for individual species in this study.

Determining whether the overlapping reflectance values observed among species are accurate involves multiple steps associated with sensors and reflectance values. The first step is calibrating the sensor before data acquisition to the brightest anticipated reflectance values. Second, ground reflectance data should be collected simultaneously with overflight acquisition to compare image reflectance values with true reflectance values. Finally, a comparison with other imagery of comparable resolution (e.g., imagery obtained in 2004 and 2005) should be done to determine whether it was the sensor or inherent environmental factors that contributed to variability in reflectance values. These last comparisons can be done before additional acquisition of four-band data.

Alternative image processing approaches might also be pursued to improve image classification accuracy. Using alternative vegetation indices such as the soil-adjusted vegetation index (which incorporates soil reflectance and normalized difference vegetation index [NDVI]) might further constrain values and help discriminate among signatures (Huete, 1988; Elvidge and Chen, 1995). Because two different NDVI filters were necessary for dark and light alluvial surfaces (appendix A), pursuing additional filters for vegetation may prove profitable. The clumped and patchy nature of vegetation along the river corridor contributes to the variability in class discrimination. When contrast and co-occurrence filters for textures were applied, which proved to be helpful in discriminating between vegetation classes, filter size had to be varied depending on vegetated stand size (appendix A). The larger dimension for texture (23-by-23 boxcar [10-m dimension]) smoothed the variations within large stands more effectively, but degraded the obvious texture of small stands by including adjacent alliance variations in the small alliance classes.

Heterogeneous plant assemblages (common in riparian communities) and scale differences between the groundtruth and image resolution also presented problems with accuracies. The 44-cm-pixel resolution provides high-resolution information that can potentially identify single individuals, but can also obscure the larger scale information on a particular cover class that may encompass 100 m² and include other interspersed species. This may be more problematic in arid environments, where cover values are low compared to eastern deciduous forests. Another mapping approach could be spectral mixture analysis (SMA), which takes into account the vegetative mosaic and may more accurately report vegetative components of the riparian community. The concept behind SMA is that the relative proportion of a few spectrally distinct elements dominates the variance observed in a remotely sensed area (Roberts and others, 1998; Elmore and others, 2000). SMA works best when the number of individual spectral signatures is smaller than the number of useful bands. For Colorado River imagery, which is limited to four bands, SMA may have limited utility. Acquiring multiple infrared bands may be necessary to improve mapping accuracy. Costs increase with the number of bands acquired, but these costs may be offset by decreasing the resolution

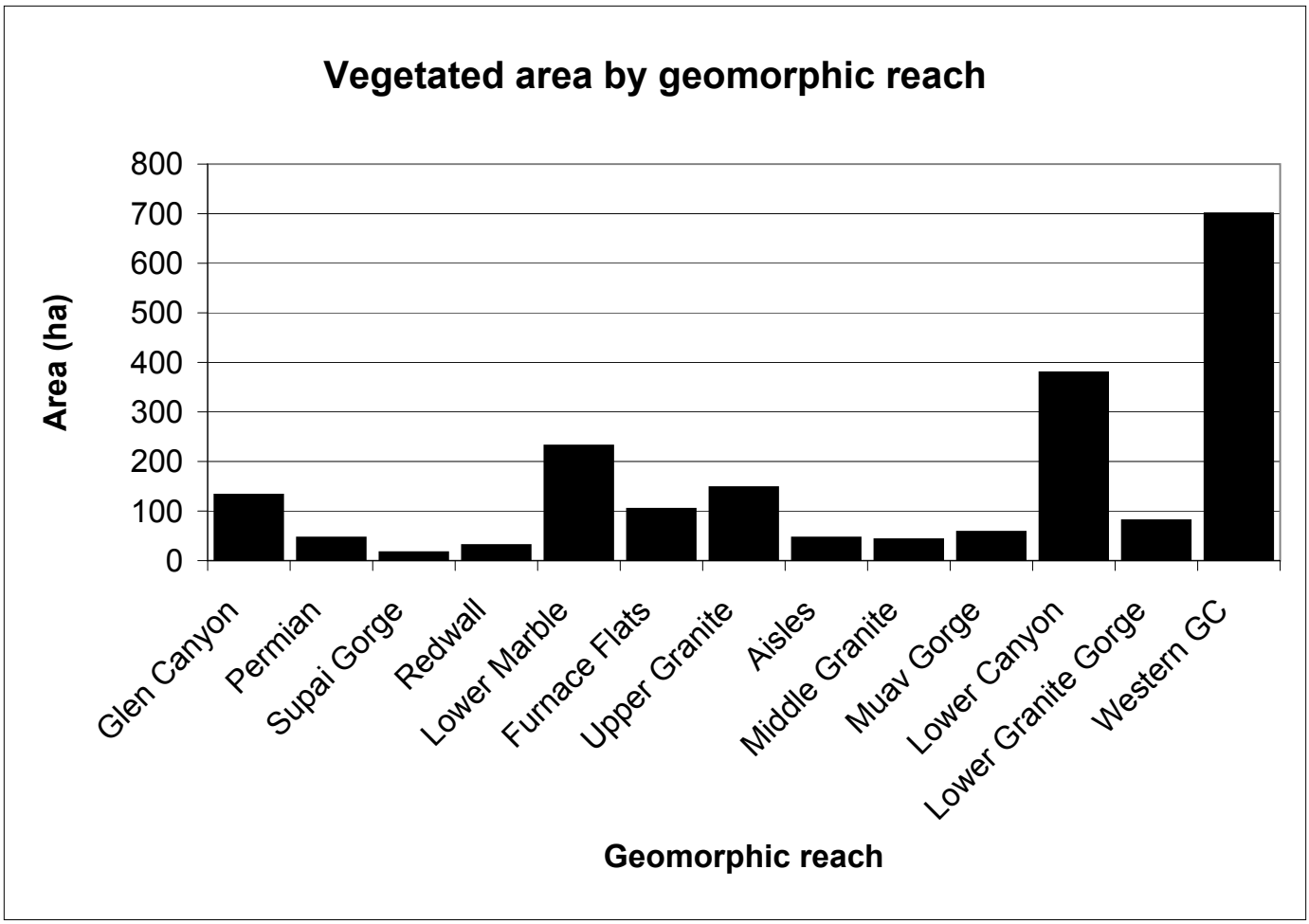

Figure 6. Total vegetated area (ha) within each geomorphic reach.

to 1 m. This needs further analysis and consideration before acquiring future imagery.

Supervised classification approaches have been effective for mapping large areas of vegetation (Eder, 1989; Mickelson and others, 1998 ; Driese and others, 2004), but these studies have also identified low accuracies for particular vegetation classes. Driese and others (2004) identified spectral similarity between beech and maple and overall accuracies of 28% for a vegetation map using multitemporal Landsat imagery. Accuracies in their study improved through aggregation of classes and use of a fuzzy accuracy assessment. Accuracies in another study (Laba and others, 2002) were higher when classes were aggregated. In this study, aggregation improved accuracy for some classes, but fuzzy dataset assessment was also used to improve the map accuracy (tables 5*A*–*C*). In a mathematical sense, the vegetation map meets national standards for mapping accuracy. The accuracy of the map for long-term change detection may be problematic beyond looking at larger scale questions about vegetated areas above a certain discharge or associated with a geomorphic feature (e.g., channel margins, debris fans).

General Changes in Vegetation

The general pattern of more vegetation in the Glen Canyon, lower Marble Canyon, Lower Canyon, and western Grand Canyon reaches (figs. 5 and 6*A*–*F*) is likely due to geomorphic and sun-aspect effects. These reaches are some of the widest and longest in the river corridor (Schmidt and Graf, 1990) and are oriented in such a manner that sun availability is also greater in these reaches than in others (Yard and others, 2005). Both available area and sunlight affect vegetation densities and areal cover. In Glen Canyon, the larger vegetated areas may also be a function of perched beaches that are less subject to erosion because of channel incision since closure of the dam (Grams and others, 2007).

The ability to compare changes in vegetation between the 2002 dataset and previous vegetation studies is limited. Although no historic data are available to determine whether this study's current areal measurement of arrowweed is an increase over time, distributional maps from Turner and Karpiscak (1980) can still be used to compare distribution data. Comparisons of distributions indicate that the range of

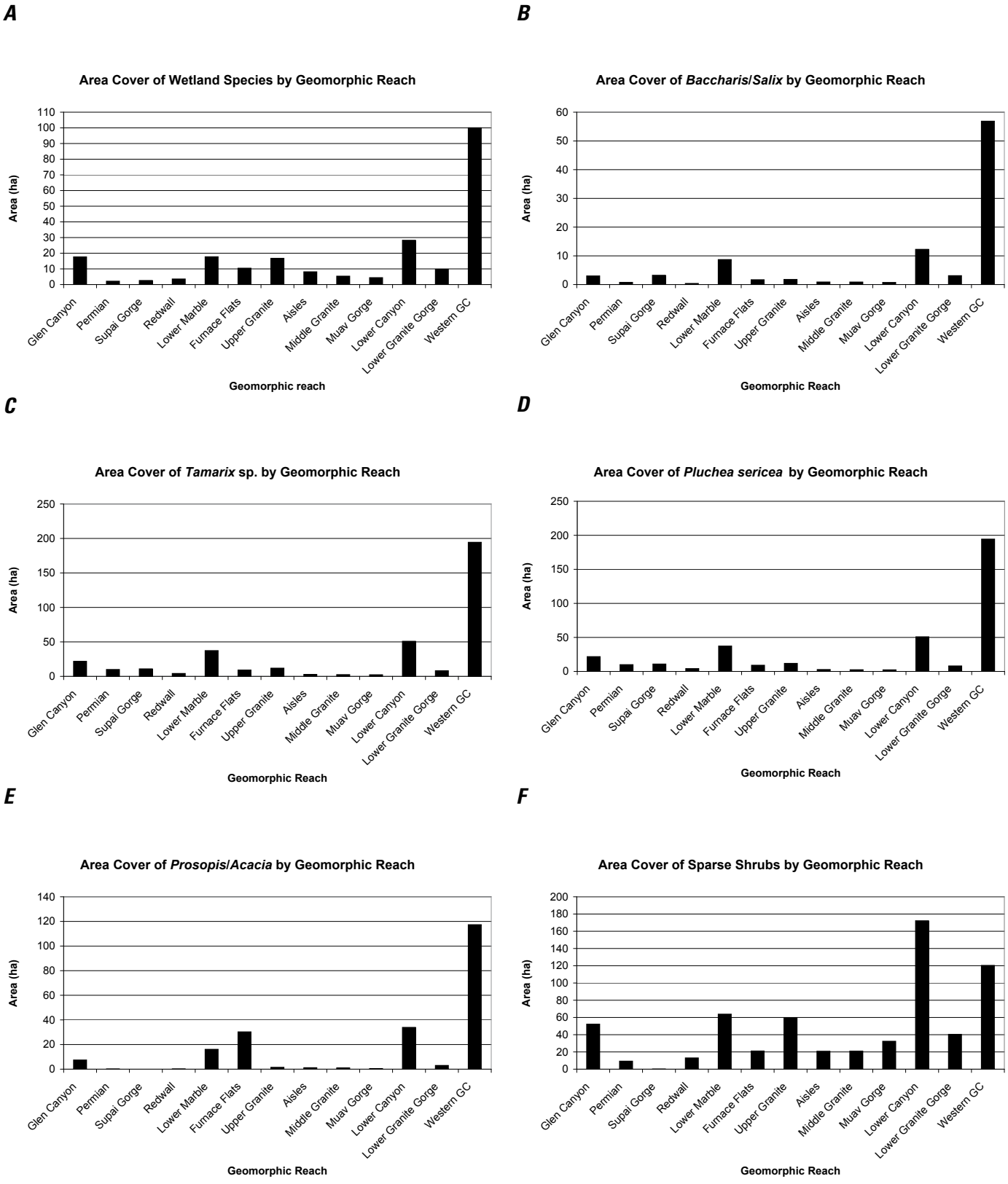

Figure 7. Areal cover of each vegetation class within each geomorphic reach. *A*, Wetlands. *B*, *Baccharis*/*Salix*. *C*, *Tamarix*. *D*, *Pluchea*. *E*, *Prosopis*/*Acacia*. *F*, Sparse shrubs.

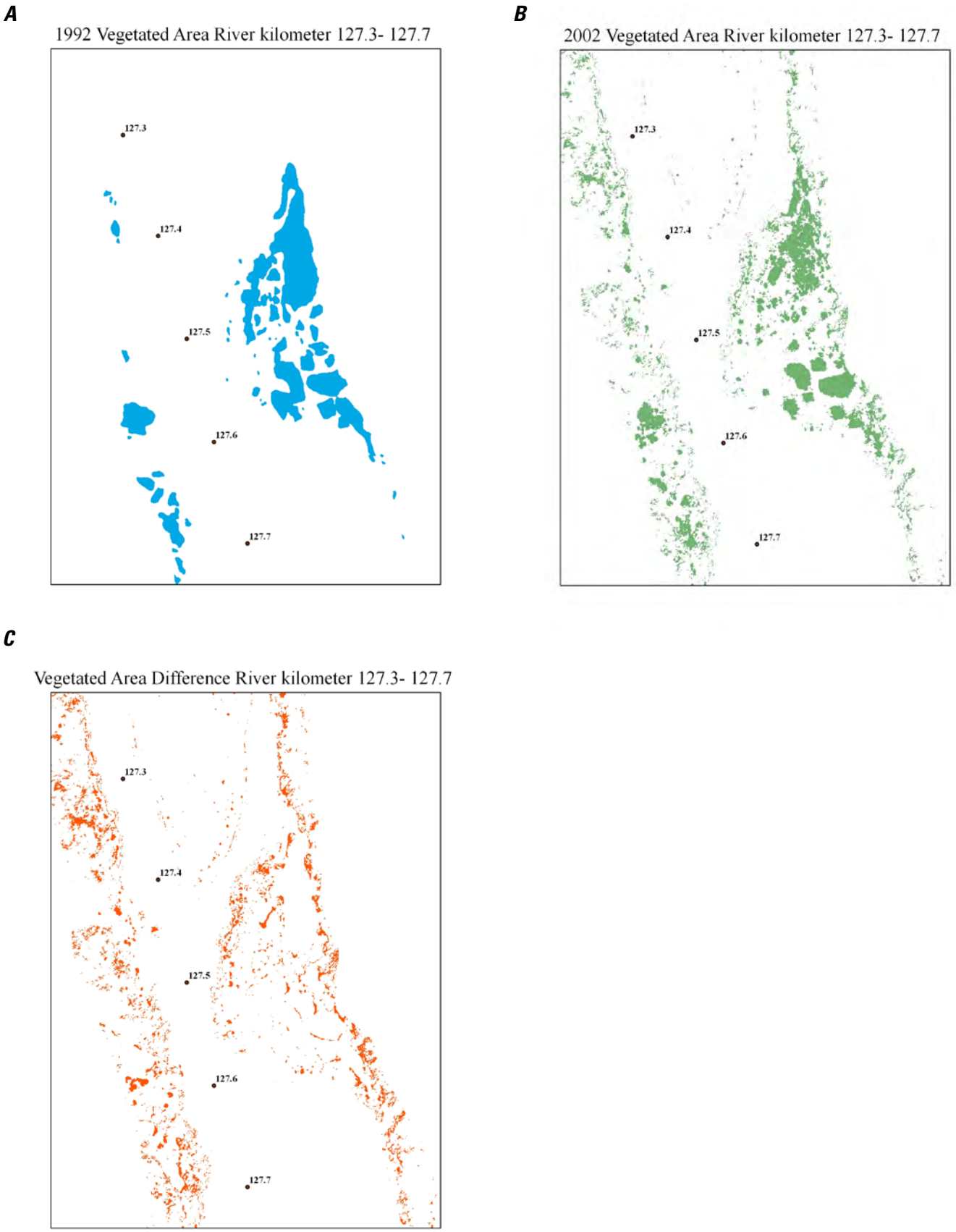

Figure 8. Vegetation cover between RK 124.9 and 127.9. *A*, 1992. *B*, 2002. *C*, The difference in vegetation between 1992 and 2002.

arrowweed has expanded upstream into Glen Canyon and is distributed more evenly within upper Marble Canyon above RK 70. These observations can be made for arrowweed, but similar observations about expansion or contraction of other species are not possible because the distribution data from 1980 were fairly general.

Areal cover comparisons with previous data are also somewhat limited because few studies identified specific vegetation classes. However, it was possible to compare mapping of a 3-km area below the Little Colorado River (RK 124–127) in 1992 with the 2002 imagery (Waring, 1995). The sparse vegetation category was not included in order to focus on large patches that provide some comparability. Using extraction programs in ArcMap, it was determined that vegetated area had increased by 6 ha in the 3-km length of river (figs. 8*A*–*C*). Rough comparisons show that the greatest increases in vegetation occurred along the shorelines of channel margins, although some previously vegetated area did expand within the debris fan area and downstream eddy bars. Waring (1995) showed that channel margins tend to gain in vegetated area over time. This comparison corroborates this pattern (fig. 8*C*), but distinct geomorphic features need to be identified to verify where vegetated area is greatest.

Admittedly, this analysis needs to go into much further detail. A better analysis may be possible if 2002 data are combined with geomorphic information previously developed by the Utah State University physical science program (principally by Jack Schmidt). In this study, only a very superficial analysis is presented to show how the 2002 vegetation map could be used to assess changes in vegetation since the last large area change detection study was conducted by Waring (1995) (these analyses are beyond the scope of this report). The limited analysis in this study indicates that riparian vegetation continues to expand within the corridor, and that systemwide vegetation inventories are critical in monitoring change in this environment. Long-term approaches for monitoring riparian vegetation should include large-scale as well as local-scale assessment of change. Further analysis is needed to determine the extent of change for other portions of the river corridor, and the types of species that have changed the most.

Map Utility for Other Resources

While the vegetation base map for the CRE provides an inventory of the area covered by vegetation, the map also has utility for integrated questions about resource change and functional linkages. Linking this map to other GIS coverages or location data provides information to stakeholders about how changes in riparian vegetation affect other resources like wildlife, campsite area, and food web linkages between terrestrial and aquatic systems. The map's initial use has been to provide annual aboveground biomass estimates within the fluctuating zone for riparian vegetation. This information can improve understanding of the contribution that local marsh and riparian vegetation make within the aquatic food webs (Kennedy and Ralston, unpub. data). Datasets associated with wildlife can also be used to begin to look at riparian vegetation and wildlife linkages. Mortenson and others (in press) made linkages between tamarisk and coyote willow occupancy and beaver locations, bringing up questions about beavers structuring riparian areas through species selection, as cited in studies outside of the CRE (Johnston and Naiman, 1990; Rosell and others, 2005). Lastly, vegetated areas can be superimposed onto campsite area maps to determine where vegetation is changing most rapidly and which riparian species are affecting camping areas the most. Kaplinski and others (2005) and Kearsley and others (1994) have pointed out that vegetation encroachment is a primary cause of campsite area decrease. Identifying these two variables can help managers target particularly vulnerable campsites and those plant species that may need to be managed through removal or trimming. Subsequent mapping could help to evaluate the success or failure of management actions, including those associated with vegetation removal.

Conclusions

The vegetation database is a critical element in assessing the status and trends of riparian vegetation for the CRE. The scale used to quantify vegetation adequately meets the needs of the stakeholder group. Increasing the scale to meet the USGS-NPS National Mapping Program's minimum mapping unit of 0.5 ha is unwarranted because this scale would reduce resolution of some classes (e.g., seep willow/coyote willow would likely be combined with tamarisk). While this would undoubtedly improve classification accuracies, it would not provide the community-level information about vegetation change that would benefit stakeholders.

Classification accuracy, which was low for some vegetation classes in this study, may be improved by increasing the spectral range of the imagery. The 2002 imagery was limited because color-infrared (green, red, and NIR) bands are limited in their ability to distinguish riparian plant species. Ensuring that image data are coregistered and that band data can be collected and accurately calibrated to capture the entire dynamic reflectance range of all plant species should improve classification. Along a similar vein, collecting multitemporal imagery may provide a means to distinguish species that have similar signatures (e.g., mesquite and salt cedar) but different phenology with respect to leaf drop (Driese and others, 2004; Schriever and Congalton, 1995). Flying two separate data collection missions, however, would likely be financially prohibitive because it would require holding releases from Glen Canyon Dam steady for the period of data acquisition (which can be several days). The identification of vegetation classes should follow NPS mapping approaches to complement the national effort and should incorporate the alternative analysis for community identification noted by Vanderhorst and others

(2007). Ensuring quality control with the contractor who is acquiring the data is also critical for the success of subsequent image processing and classification.

The sparse nature of semiarid to arid environments and the heterogeneous nature of riparian habitats pose additional mapping challenges. Vegetation classes like shrubs and bunch grasses that may be ecologically distinct could not be separately identified with confidence using only species assemblage data. The small leaf areas and sparse occurrences of these communities make them difficult to distinguish digitally. On the other hand, the dense and somewhat heterogeneous nature of riparian vegetation made it equally difficult to digitally distinguish the boundaries between *Tamarix* and other riparian overstory classes like *Baccharis emory-Salix exigua*. Other researchers (Ohmann and Gregory, 2002; Schmidtlein and Sassin, 2004) have used remotely sensed data in combination with environmental parameters to improve mapping accuracies. Within the CRE, additional parameters that could be explored to improve accuracies of heterogeneous species classification are stage elevation data (e.g., marsh vegetation would generally be below 708 m^3/s) to restrict classification choices in an automated process; inclusion of ecological parameters; the use of SMA to estimate the fractional cover of species within each pixel (Roberts and others, 1998) and better quantify the cover of individual species composing a cover class; slope aspect with respect to solar illumination to further define plant distributions in combination with remotely sensed data (Walton and others, 2005); and object-based classification software used in combination with these suggestions (Lindsey and Donnelly, 2006). Photo-interpretation may not be feasible for use due to time and cost constraints. Geographic distribution may be another parameter to consider, but if plant ranges are contracting or expanding, limiting geographic distribution may exclude the identification of this phenomenon.

This map database provides a base layer associated with vegetative cover that can be used in combination with other existing GIS coverages to make linkages among terrestrial and aquatic resources. The linkage between campsites and vegetation encroachment can be monitored over time using this and subsequent vegetation area maps. Habitat and terrestrial vertebrate and invertebrate linkages can also begin to be made with this map. The vegetation base map also provides shoreline vegetation information that may be used in fisheries projects associated with shoreline habitat. The additional benefits of this product will become more evident as other resources use the information and as subsequent vegetation databases are produced for monitoring long-term change.

Acknowledgments

Funding for this work was provided through the Glen Canyon Dam Adaptive Management Program. Cooperative agreements between USGS/GCMRC and Northern Arizona University (99HQAG0175 cooperative project award 99175HS021) and between USGS/GCMRC and Pinnacle Mapping Technologies, Inc (Agreement Number 03WRAG0004) ensured the completion of data collection and image processing. We thank Carol Fritzinger, GCMRC, for her logistic coordination, and river guides Dave Baker, Jeff Behan, Steve Jones, Dirk Pratley, Lynn Roeder, J.P. Running, and Brian Smith (provided through Humphrey Summit Support) for their assistance and patience as they navigated our way to the sampling sites and through the canyon without incident. Matthew Andersen, David Salas, and two anonymous reviewers provided constructive comments that improved this document. Patty McCredie provided valuable editorial assistance that improved the appearance and readability of this document.

References

Anderson, L.S., and Ruffner, G.A., 1987, Effects of the post-Glen Canyon Dam flow regime on the old high water line plant community along the Colorado River in Grand Canyon: Glen Canyon Environmental Studies, executive summaries of technical reports, NTIS no. PG-183504/AS.

Ares, J., del Valle, H, Bisigato, A., 2003, Detection of process-related changes in plant patterns at extended spatial scales during early dryland desertification: Global Change Biology, v. 9, p. 1643–1659.

Ayers, T.J., Scott, R.W., Stevens, L.E., Warren, K., Phillips, A.M., III, and Yard, M.E., 1994, Additions to the flora of the Grand Canyon National Park—I.: Journal of the Arizona-Nevada Academy of Science, v. 29, p. 70–75.

Bestelmeyer, B.T., Trujillow, D.A., Tugel, A.J., Havstad, K.M., 2006, A multi-scale classification of vegetation dynamics in arid lands: What is the right scale for models, monitoring, and restoration?: Journal of Arid Environments, v. 65, p. 296–318.

Brian, N.J., 2000, A field guide to the special status plants of Grand Canyon National Park: Science Center, Grand Canyon National Park, Grand Canyon, Ariz.

Brown, D.E., 1982, Biotic communities of the American Southwest—United States and Mexico: Desert Plants, v. 4. nos. 1–4.

Carothers, S.W., and Aitchison, S.W., eds., 1976, An Ecological survey of the riparian zone of the Colorado River between Lees Ferry and the Grand Wash Cliffs, Arizona: Final report to U.S. Department of the Interior, National Park Service, Grand Canyon National Park, Ariz., 251 p.

Clover, E.U., and Jotter, L., 1944, Floristic studies in the canyon of the Colorado and tributaries: American Midland Naturalist, v. 32, p. 591–642.

Congalton, R.G., 1991, A review to assess the accuracy of classifications of remotely sensed data: Remote Sensing of Environment, v. 37, p. 35–46.

Driese, K.L., Reiners, W.A., Lovett, G.M., and Simkins, S.M., 2004, A vegetation map for the Catskill Park, NY, derived from multi-temporal Landsat imagery and GIS data: Northeastern Naturalist, v. 11, p. 421–442.

Duncan, J., Stow, D., Franklin, J., and Hope, A., 1993, Assessing the relationship between spectral vegetation indices and shrub cover in the Jornada Basin, New Mexico: International Journal of Remote Sensing, v. 14, p. 3395–3416.

Eder, J.J., 1989, Don't shoot unless it's autumn: Journal of Forestry, v. 87, p. 50–51.

Elmore, A.J., Mustard, J.F., Manning, S.J., and Lobell, D.B., 2000, Quantifying vegetation change in semiarid environments: precision and accuracy of spectral mixture analysis and the normalized difference vegetation index: Remote Sensing of Environment, v. 73, p. 87–102.

Elvidge, C.D., and Chen, Z., 1995, Comparison of broad-band and narrow-band red and near-infrared vegetation indices: Remote Sensing of Environment, v. 54, p. 38–48.

Ehleringer, J., 1981, Leaf absorptances of Mohave and Sonoran Desert plants: Oecologia, v. 49, p. 366–370.

ENVI Image Analysis Software, 2006, v4.2. ITT Visual Information Solutions©: Boulder, Colo.

ESRI©, 2005, ArcMap™ v. 9.1: Redlands, Calif.

Farley, G.H., Ellis, L.M., Stuart, J.N., and Scott, N.J., Jr., 1994, Avian species richness in different-aged stands of riparian forest along the middle Rio Grande, New Mexico: Conservation Biology, v. 8, p. 1098–1108.

Federal Geographic Data Committee Vegetation Subcommittee, 1997, Vegetation classification standard: Federal Geographic Data Committee, 58 p., http://www.fgdc.gov/standards/projects/FGDC-standards-projects/vegetation/vegclass.pdf, accessed June 18, 2008.

Fradkin, P.L., 1984, A river no more: The Colorado River and the West: Tucson, Ariz., The University of Arizona Press, 360 p.

Gopal, S., and Woodcock, C., 1994, Theory and methods of accuracy assessment using fuzzy sets: Photogrammetric Engineering and Remote Sensing, v. 60, p. 181–188.

Grams, P.E., Schmidt, J.C., and Topping, D.J., 2007, The rate and pattern of bed incision and bank adjustment on the Colorado River in Glen Canyon downstream from Glen Canyon Dam, 1956–2000: Geological Society of America Bulletin, v. 119, p. 556–575.

Grossman D.H., Faber-Langendoen D., Weakley A.S., Anderson M., Bourgeron P., Crawford R., Goodin K., Landaal S., Metzler K., Patterson K.D., Pyne M., Reid M., and Sneddon L. 1998. International classification of ecological communities: terrestrial vegetation of the United States. Volume I, The National Vegetation Classification Standard: development, status, and applications. The Nature Conservancy: Arlington, VA.

Hansen, M., Coles, J., Thomas, K.A., Cogan, D., Reid, M., Von Loh, J., and Schulz, K., 2004, USGS-NPS Vegetation Mapping Program: Walnut Canyon National Monument, Arizona, vegetation classification and distribution: U.S Geological Survey, Southwest Biological Science Center, Flagstaff, Ariz., 86 p.

Herbel, C.H., Ares, F.N., Wright, R.H., 1972, Drought effects on a semidesert grassland range: Ecology, v. 53, p. 1084–1093.

Hill, M.O., 1979, TWINSPAN—a FORTRAN program for arranging multivariate data in an ordered two-way table by classification of the individuals and attributes: Microcomputer Power, Ithaca, N.Y.

Howe, M.M., 2001, Effects of regulation on the wetland seed bank along the Colorado River in Grand Canyon: Masters thesis, Northern Arizona University, Flagstaff, Ariz.

Huete, A.R., and Jackson, R.D., 1988, Soil and atmosphere influences on the spectra of partial canopies: Remote Sensing of Environment, v. 25, p. 89–105.

Hurcom, S.J., and Harrison, A.R., 1998, The NDVI and spectral decomposition for semi-arid vegetation abundance estimation: International Journal of Remote Sensing, v. 19, p. 3109– 3125.

Johnson, R.R., Haight, L.T., and Simpson, J.M., 1977, Endangered species vs. endangered habitats—a concept, in Johnson, R.R., and Jones, D.A., Jr., technical coordinators, Importance, preservation and management of riparian habitat: a symposium: USDA Forest Service General Technical Report RM-43, p. 68–79.

Johnston, C.A., and Naiman, R.J., 1990, Browse selection by beaver: effects on riparian forest composition: Canadian Journal of Forest Research, v. 20, p. 1036–1043.

Kaplinski, M., Hazel, J., and Parnell, R., 2005, Campsite area monitoring in the Colorado river ecosystem: 1998 to 2003: Final report to Grand Canyon Monitoring and Research Center, U.S. Geological Survey, from Northern Arizona University, Flagstaff, Ariz., 39 p.

Kearsley, L.H., Schmidt, J.C., and Warren, K.D., 1994, Effects of Glen Canyon Dam on Colorado River sand deposits used as campsites in Grand Canyon National Park, USA: Regulated Rivers: Research and Management, v. 9, p. 137–149.

Kearsley, M.J.C., 2006, Vegetation dynamics, in Kearsley, M.J.C. ed., Inventory and monitoring of terrestrial riparian resources in the Colorado River corridor of the Grand Canyon: an integrative approach: Final report from Northern Arizona University submitted to the Grand Canyon Monitoring and Research Center, U.S. Geological Survey, Flagstaff, Ariz., 218 p.

Kearsley, M.J.C., and Ayers, T.J., 1996, The effects of interim flows from Glen Canyon Dam on riparian vegetation in the Colorado River corridor, Grand Canyon National Park, Arizona: Final report from Northern Arizona University submitted to the Grand Canyon Science Center, Grand Canyon National Park, Grand Canyon, Ariz., 40 p.

Kearsley, M.J.C., and Ayers, T.J., 1999, Riparian vegetation responses: snatching defeat from the jaws of victory and vice versa, in Webb, R.H., Schmidt, J.C., Marzold, G.R., and Valdez, R.A., eds., The controlled flood in Grand Canyon: Washington, D.C., American Geophysical Union, Geophysical Monograph Series, v. 110, p. 309–327.

Kearsley, M.J.C., Cobb, N., Yard, H., Lightfoot, D., Brantley, S., Carpenter, G., and Frey J., 2006, Inventory and monitoring of terrestrial riparian resources in the Colorado River corridor of the Grand Canyon: an integrative approach: Final report from Northern Arizona University submitted to the Grand Canyon Monitoring and Research Center, U.S. Geological Survey, Flagstaff, Ariz., 218 p.

Klopfer, S.D., Olivero, A., Sneddon L., and Lundgren, J., 2002, Final report of the NPS Vegetation Mapping Program Fire Island National Seashore: Conservation Management Institute, GIS and Remote Sensing Division, Virginia Tech. Blacksburg, Va.

Laba, M.L., Gregory, S., Braden, J., Ogurcak, D., Hill, E., Fegraus, E., Fiore, J., and DeGloria, S.D., 2002, Conventional and fuzzy accuracy assessment of the New York Gap Analysis Project land cover map: Remote Sensing of Environment, v. 82, p. 443–456.

Lindsey, D., and Donnelly, P., 2006, Vegetation Habitat Mapping: Object Based Image Classification Using SPRING Software: U.S. Fish and Wildlife Service NWR Remote Sensing Laboratory, Division of Planning, Albuquerque, N. Mex., http://www.fws.gov/data/documents/SPRING%20Manual%20022306.pdf, accessed February 22, 2008.

McCune, B., and Grace, J.B., 2002, Analysis of ecological communities: MjM Software Design, Gleneden Beach, Oreg., 300 p.

McCune, B., and Mefford, M.J., 1999, Multivariate analysis of ecological data, version 4.01, MjM Software, Gleneden Beach, Oreg.

Mickelson, J.G., Civco, D.L, and Silander, J.A., 1998, Delineating Forest canopy species in the northeastern United States using multi-temporal TM imagery: Photogrammetric Engineering and Remote Sensing, v. 64, p. 891–904.

Montgomery, D.R., and MacDonald L.H., 2002, Diagnostic approach to stream channel assessment and monitoring: Journal of the American Water Resources Association, v. 38, p. 1–16.

Mooney, H.A., Ehleringer, J., and Björkman, O., 1977, The energy balance of leaves of the evergreen desert shrub Atriplex hymenelytra: Oecologia, v. 29, p. 301–310.

Mortenson, S.G, Weisberg, P.J., and Ralston, B.E., in press, Do beavers promote the invasion of non-native *Tamarix* in the Grand Canyon riparian zone?: Wetlands.

Naiman, R.J., Decamps, H., eds., 1990, The ecology and management of aquatic-terrestrial ecotones: Paris: United Nations Educational, Scientific and Cultural Organization, Park Ridge: Parthenon.

Naiman, R.J., Decamps, H., McClain, M.E., 2005, Riparia: Ecology, conservation and management of streamside communities: Burlington, Mass., Elsevier Academic Press.

The Nature Conservancy, 1994, Field methods for vegetation mapping: for the U.S. Department of the Interior National Biological Survey and National Park Service, 196 p., http://biology.usgs.gov/npsveg/ftp/vegmapping/field_methods/title.doc, accessed June 18, 2008.

Ohmann, J.L., and Gregory, M.J., 2002, Predictive mapping of forest composition and structure with direct gradient analysis and nearest neighbor imputation in coastal Oregon, USA: Canadian Journal of Forest Research, v. 32, p. 725–741.

Phillips, B.G., Phillips, A.M., III, and Schmidt-Bernzott, M.A., 1987, Annotated checklist of vascular plants of Grand Canyon National Park: Grand Canyon Natural History Assoc. Monograph No. 7, 79 p.

Phillips, B.G, Phillips, A.M., III, Theroux, M., and Downs, J., 1977, Riparian vegetation of Grand Canyon National Park, Arizona: Report to Grand Canyon National Park, 200 p.

Porter, M.E., 2002, Riparian vegetation responses to contrasting managed flows of the Colorado River in Grand Canyon, Arizona: Masters thesis, Northern Arizona University.

Ralston, B.E., 2005, Riparian vegetation and associated wildlife, in Gloss, S.P, Lovich, J.E., and Melis, T.S., eds., The State of the Colorado River ecosystem in Grand Canyon: U.S. Geological Survey Circular 1282, p. 103–122.

Roberts, D.A., Gardner, M., Chruch, R., Ustin, S., Scheer, G., and Green, R.O., 1998, Mapping chaparral in the Santa Monica Mountains using multiple endmember spectral mixture models: Remote Sensing of Environment, v. 65, p. 267–279.

Rosell, F., Bozser, O., Collen, P., and Parker, H., 2005, Ecological impact of beavers Castor fiber and Castor canadensis and their ability to modify ecosystems: Mammal Review, v. 35, p. 248–276.

Schmidt, J.C., 1990, Recirculating flow and sedimentation in the Colorado River in Grand Canyon, Arizona: Journal of Geology, v. 98, p. 709–724.

Schmidt, J.C., and Graf, J.B., 1990, Aggradation and degradation of alluvial-sand deposits, 1965 to 1986, Colorado River, Grand Canyon National Park, Arizona: U.S. Geological Survey Professional Paper 1493.

Schmidtlein, S., and Sassin, J., 2004, Mapping of continuous floristic gradients in grasslands using hyperspectral imagery: Remote Sensing of Environment, v. 92, p. 126–138.

Schriever, J.R., and Congalton, R.G., 1995, Evaluating seasonal variability as an aid to cover-type mapping from Landsat Thematic Mapper data in the northeast: Photogrammetric Engineering and Remote Sensing, v. 61, p. 321–327.

Stevens, L.E., 1989, Mechanisms of riparian plant community organization and succession in the Grand Canyon, Arizona: Ph.D. Dissertation, Northern Arizona University, Flagstaff, Ariz.

Stevens, L.E., and Ayers, T.J., 1993, The impacts of Glen Canyon Dam on riparian vegetation and soil stability in the Colorado River corridor, Grand Canyon, Arizona: 1992 Final report. Report submitted to National Park Service Cooperative Studies Unit, Northern Arizona, Flagstaff, Ariz.

Stevens, L.E., and Ayers, T.J., 1997, Effects of interim flows from Glen Canyon Dam on fluvial marshes of lower Glen Canyon, Arizona: Final report. Report submitted to U.S. Geological Survey, Biological Resources Division, Flagstaff, Ariz.

Stevens, L.E., Ayers, T.J., Bennett, J.B., Christensen, K., Kearsley, M.J.C., Meretsky, V.J., Phillips, A.M., III, Parnell, R.A., Spence, J., Sogge, M.K., Springer, A.E., and Wegner, D.L., 2001, Planned flooding and Colorado River riparian trade-offs downstream from Glen Canyon Dam, Arizona: Ecological Applications, v. 11, p. 701–710.

Stevens, L.E., Schmidt, J.C., Ayers, T.J., and Brown, B.T., 1995, Flow regulation, geomorphology, and Colorado River marsh development in the Grand Canyon, Arizona: Ecological Applications, v. 5, p. 1025–1039.

Stromberg, J.C., Tiller, R., and Richter, B., 1996, Effects of groundwater decline on riparian vegetation of semiarid regions: the San Pedro, Arizona: Ecological Applications, v. 6, p. 113–131.

Topping, D.J., Schmidt, J.C., and Vierra, L.E., Jr., 2003, Computation and analysis of the instantaneous-discharge record for the Colorado River at Lees Ferry, Arizona – May 8, 1921, through September 30, 2000: U.S. Geological Survey Professional Paper Series 1677, 59 p.

Turner, R.M., and Karpiscak, M.M., 1980, Recent vegetation changes along the Colorado River between Glen Canyon Dam and Lake Mead, Arizona: U.S. Geological Survey Professional Paper 1132, 125 p.

Urquhart, N.S., Auble, G.T., Blake, J.G., Bolger, D.T., Gerrodette, T., Leibowitz, S.G., Lightfoot, D.C., and Taylor, A.H., 2000, Report of a peer review panel on terrestrial aspects of the biological resources program of the Grand Canyon Monitoring and Research Center: Report to Grand Canyon Monitoring and Research Center, U.S. Geological Survey, Flagstaff, Ariz., 54 p.

U.S. Department of Interior, 1996, Record of Decision, Operations of Glen Canyon Dam Final Environmental Impact Statement: Washington, D.C., Office of the Secretary of Interior, 15 p.

Vanderhorst, J.P., Jeuck, J., and Gawler, S.C., 2007, Vegetation classification and mapping of New River Gorge National River: West Virginia. Technical Report NPS/NER/NRTR 2007/092, National Park Service, Philadelphia, Pa.

Walton, J.C., Martinez-Gonzales, F., and Worthington, R., 2005, Desert vegetation and timing of solar radiation: Journal of Arid Environments, v. 60, p. 697–707.

Waring, G.L., 1995, Current and historical riparian vegetation trends in Grand Canyon, using multitemporal remote sensing analyses of GIS sites: Final report, National Park Service, 24 p.

Waring, G.L., and Stevens, L.E., 1986, The effects of recent flooding on riparian plant establishment in Grand Canyon: Glen Canyon Environmental Studies, executive summaries of technical reports, NTIS no. PB-183496.

Westhoff, V., and van der Maarel, E., 1978, The Braun-Blanquet approach, in Whittaker, R.H., ed., Classification of plant communities, Junk, The Hague, 408 p.

Yard, M.D., Bennett, G.E., Mietz, S.N., Coggins, L.G., Stevens, L.E., Hueftle, S., and Blinn, D.W., 2005, Influence of topographic complexity on solar insolation estimates for the Colorado River, Grand Canyon AZ: Ecological Modeling, v. 183, p. 157–182.

Appendix A. Image Processing

Image Band Calibration

Ground reflectance data obtained in the year 2000 were used to determine the gain (digital number [DN]/reflectance) and offset or bias (DN) for each color band. Reflectance is the ratio of the reflected solar energy to the incident solar energy; a reflectance value of 1.0 indicates a perfect reflector. The vegetation alliances used in these calibrations are listed in table A1; sand, alluvium, litter, concrete, asphalt, and tin were also used, where they existed within the ISTAR data for the Colorado River ecosystem (CRE). The recorded image values and ground reflectance values used in this study for calibrations are listed in tables A2–A5 for the four regions where ground information was collected. The resulting calibrations for sets of flight zones are summarized in tables A6*A–F*. Examination of these DN-reflectance relations shows that the near-infrared (NIR) band data are saturated at high DN at about 40%–45% reflectance (table A6E). Thus, certain vegetation alliances that have high reflectance values in the NIR probably have similar DN, which makes their discrimination more difficult. The other three color bands and the panchromatic band display an unsaturated linear relation with ground reflectance.

The radiometric calibrations derived for each color band within four sets of flight zones showed a fairly narrow range in gain (table A7), with the gains for the blue, green, and panchromatic bands varying by 4.0% or less, and those for the red and NIR bands varying 8.1%–9.8%. The gain value for the panchromatic band is much larger than those for the color bands because the panchromatic band data are 12-bit values (0–4,095), whereas the color bands were recorded as 8-bit (0–255) values. These average gain values were used to determine each band's offsets within each set of flight zones by least squares analysis. The offsets represent the DN value at zero reflectance, which indicates the amount of atmospheric scattering at a particular wavelength and flight zone. The derived offset values within the four sets of flight zones have a narrow range (table A7) and were considered to be essentially constant throughout the corridor.

Image Data Masks

Several data masks were produced and used in the analysis of the image data to map vegetation. Two primary masks were generated to restrict the study area within the CRE to the region between the water's edge and the landward limit of 80,000-cfs (2,265-m3/s) river flow level. The water's edge was manually digitized using the ISTAR image data and used to exclude water. Normally, a water mask can easily be produced using the distinctive low, flat reflectance spectra

Table A1. Preliminary vegetation classes and number of ground spectroradiometric readings taken in the field.

Vegetation class	Species name or description of class	Number of samples
ATCA	*Atriplex canescens*	22
BAXX	*Baccharis spp.*	36
CERE	*Celtis reticulata*	32
EQFE	*Equisetum ferrisii*	16
IMBR	*Imperata brevifolia*	29
LATR	*Larrea tridentata*	19
PHAU	*Phragmites australis*	28
PLSE	*Pluchea sericea*	17
PRGL	*Prosopis glandulosa*	28
QUTU	*Quercus turbinella*	34
SAEX	*Salix exigua*	27
SAGO	*Salix goodingii*	39
TARA	*Tamarix ramossisima*	28
TYDO	*Typha domingensis*	36
WTLD	Wetland grasses and sedges	29
BDRX/SAND	Bedrock/sand	10
Dead grass	Litter	4
Dead brush	Litter	17

Table A2. ISTAR color-band data and ground spectroradiometric data for various materials that occur within the flight line zones 1 and 2. Ground reflectance data were convolved to the band wavelengths of the ISTAR CCD sensors.

Zones 1b and 2	B1	B2	B3	B4	PAN
			Image (digital number)		
LITTER_2	79.0	67.7	70.3	73.6	897.3
ASPHALT	88.8	83.6	85.0	78.2	1091.1
LITTER_2	114.1	109.6	106.2	104.9	1363.0
8_6 TERR ALLUV	135.9	150.9	161.0	167.3	2009.0
ATCA	106.5	111.4	100.9	155.9	1449.8
TARA	71.5	90.2	70.5	168.4	1177.6
CERE	67.8	84.1	73.1	223.4	1265.2
CONCRETE	213.8	222.0	208.2	163.1	2675.0
20_1 TERR ALLUV_2	191.1	198.0	206.9	200.5	2636.6
SAEX	73.4	86.4	72.4	238.0	1319.9
SAND_2	222.0	232.1	226.7	223.8	2976.9
8_5 BEACH SAND	221.1	236.1	231.9	233.1	2895.1
14_3 BEACH SAND	221.7	239.1	229.7	224.8	2887.6
PHAR	68.4	80.9	62.5	241.5	1222.7
PHAR	64.2	83.0	74.5	251.6	1437.0
SEDGES	65.9	82.3	74.6	235.7	1416.1
CERE_2	73.0	96.0	78.0	241.0	1493.0
			Ground (reflectance)		
LITTER_2	0.0425	0.0471	0.0548	0.0671	0.0538
ASPHALT	0.0588	0.0723	0.0901	0.1040	0.0844
LITTER_2	0.0776	0.1000	0.1390	0.1941	0.1321
8_6 TERR ALLUV	0.1198	0.1662	0.2376	0.2781	0.2206
ATCA	0.0704	0.1090	0.1148	0.3002	0.1451
TARA	0.0541	0.0954	0.0856	0.3191	0.1298
CERE	0.0544	0.1044	0.4840	0.3380	0.1210
CONCRETE	0.2157	0.2525	0.3165	0.3514	0.2966
20_1 TERR ALLUV_2	0.1682	0.2276	0.3207	0.3683	0.2984
SAEX	0.0717	0.1063	0.0796	0.3864	0.1395
SAND_2	0.1828	0.2574	0.3750	0.4551	0.3497
8_5 BEACH SAND	0.1828	0.2574	0.3750	0.4551	0.3497
14_3 BEACH SAND	0.1828	0.2574	0.3750	0.4551	0.3497
PHAR	0.0459	0.0987	0.0582	0.5215	0.1432
PHAR	0.0459	0.0987	0.0582	0.5215	0.1432
SEDGES	0.0272	0.0899	0.0379	0.5770	0.1432
CERE_2	0.0648	0.1208	0.0692	0.5874	0.1722

Table A3. ISTAR color-band data and ground spectroradiometric data for various materials that occur within the flight line zones 4 and 5. Ground reflectance data were convolved to the band wavelengths of the ISTAR CCD sensors.

Zones 4 and 5	B1	B2	B3	B4	PAN
	Image (digital number)				
LITTER_4	96.0	92.0	95.0	100.0	1172.0
LITTER_5a	90.0	87.0	86.0	93.0	1247.0
LITTER_5b	88.3	82.4	90.6	93.6	1279.1
PLSE_DARK_5a	95.3	87.6	90.3	99.4	1343.3
PLSE_RED_5a	96.7	95.7	94.0	132.1	1476.2
ATCA?_5a	112.1	108.1	115.6	162.1	1715.7
ATCA2?_5a	95.6	102.7	113.0	176.9	1737.1
PRGL_5b	58.3	66.3	68.9	178.5	1177.4
PRGL_DARK_5a	72.8	81.6	71.6	211.5	1359.4
NANK DARK BROUND CHANNEL_5a	194.5	204.6	235.0	231.6	2785.6
NANK RED SAHLYDIRT_5a	202.7	211.2	234.6	232.4	2664.3
SADDLE RED WADI_5a	134.9	158.4	229.2	242.6	2630.4
PLSE_4	102.7	108.5	95.3	219.6	1445.9
SAEX_4	79.5	91.3	77.6	244.5	1338.9
SAEX_5a_DARK	120.4	132.6	114.8	187.3	1804.9
NANK SAND_5a	237.0	237.5	239.7	234.5	2944.5
SAND_4	237.9	244.1	245.2	241.6	2997.0
SAND_5a	232.8	237.1	243.8	240.8	3045.1
SAND_5b	232.0	235.4	240.5	236.0	2986.4
TARA_4	80.3	89.7	76.8	237.8	1230.1
TARA_5a	66.0	81.3	62.8	226.6	1356.0
PRGL RED_5a	61.3	67.7	49.5	209.9	1163.4
SAEX_5a-RED	79.8	92.0	80.5	222.3	1544.2
SAEX-HIGHER_5b	63.1	88.0	77.0	253.0	1533.0
BASL_5b	60.7	73.8	72.3	223.7	1327.0
PHAR_4	79.4	92.1	79.5	242.8	1317.2
PHAR_5a	60.8	78.9	63.7	244.7	1405.5
PHAR_5b	53.9	70.5	68.7	250.2	1341.1
TYDO_5a	60.4	77.2	59.6	250.2	1371.0
TYDO_5b	63.6	79.5	72.1	252.3	1428.1
WATERCRESS	88.0	112.0	80.0	254.0	1659.0

Table A3. ISTAR color-band data and ground spectroradiometric data for various materials that occur within the flight line zones 4 and 5. Ground reflectance data were convolved to the band wavelengths of the ISTAR CCD sensors.—Continued.

Zones 4 and 5	B1	B2	B3	B4	PAN
	Ground (reflectance)				
LITTER_4	0.0645	0.0804	0.1063	0.1393	0.1017
LITTER_5a	0.0645	0.0804	0.1063	0.1393	0.1017
LITTER_5b	0.0645	0.0804	0.1063	0.1393	0.1017
PLSE_DARK_5a	0.0645	0.0804	0.1063	0.1393	0.1017
PLSE_RED_5a	0.0669	0.0918	0.1097	0.2037	0.1250
ATCA?_5a	0.0704	0.1090	0.1148	0.3002	0.1600
ATCA2?_5a	0.0704	0.1090	0.1148	0.3002	0.1600
PRGL_5b	0.0487	0.0830	0.0583	0.3325	0.1116
PRGL_DARK_5a	0.0497	0.0977	0.0602	0.3484	0.1263
NANK DARK BROUND CHANNEL_5a	0.1682	0.2276	0.3207	0.3683	0.2984
NANK RED SAHLYDIRT_5a	0.1682	0.2276	0.3207	0.3683	0.2984
SADDLE RED WADI_5a	0.1098	0.1593	0.3135	0.3841	0.2758
PLSE_4	0.0714	0.1060	0.0795	0.3854	0.1392
SAEX_4	0.0717	0.1063	0.0796	0.3864	0.1395
SAEX_5a_DARK	0.0841	0.1376	0.0889	0.3980	0.1632
NANK SAND_5a	0.1972	0.2675	0.3683	0.4173	0.3434
SAND_4	0.1972	0.2675	0.3683	0.4173	0.3434
SAND_5a	0.1972	0.2675	0.3683	0.4173	0.3434
SAND_5b	0.0438	0.2675	0.3683	0.4173	0.3434
TARA_4	0.0438	0.0911	0.0581	0.4235	0.1304
TARA_5a	0.0427	0.0911	0.0581	0.4235	0.1304
PRGL RED_5a	0.0476	0.0797	0.0453	0.4238	0.1185
SAEX_5a-RED	0.0476	0.1154	0.0852	0.4271	0.1588
SAEX-HIGHER_5b	0.0335	0.1154	0.0852	0.4271	0.1588
BASL_5b	0.0459	0.0768	0.0470	0.4377	0.1205
PHAR_4	0.0459	0.0987	0.0582	0.5215	0.1432
PHAR_5a	0.0459	0.0987	0.0582	0.5215	0.1432
PHAR_5b	0.0383	0.0987	0.0582	0.5215	0.1432
TYDO_5a	0.0383	0.0870	0.0436	0.5423	0.1370
TYDO_5b	0.0000	0.0870	0.0436	0.5423	0.1370
WATERCRESS	0.0527	0.1196	0.0710	0.5664	0.1767

Table A4. ISTAR color-band data and ground spectroradiometric data for various materials that occur within the flight line zones J, K, and L. Zones are further divided into segments defined by lower case letters (eg., Ja, La). Ground reflectance data were convolved to the band wavelengths of the ISTAR CCD sensors.

Zones Jd, K, La	B1	B2	B3	B4	PAN
			Image (digital number)		
LITTER_K	83.1	74.9	76.4	80.6	978.4
LATR_K	73.6	68.6	76.1	92.8	984.9
LATR_La	94.3	85.8	88.4	104.8	1066.6
LITTER	104.8	100.0	105.0	105.8	1139.1
LATR	104.3	102.0	105.5	126.9	1257.1
PRGL	66.0	71.8	62.9	193.1	934.5
CERE	70.9	78.8	64.6	213.1	1007.6
SAEX	77.6	93.8	72.7	236.7	1209.5
SAND	239.3	241.8	243.1	241.2	2849.9
SAND_K	241.9	244.1	246.7	246.2	2612.4
SAND_La	243.8	247.1	248.8	247.0	2869.5
SAEX_K	156.6	169.4	162.2	236.3	1775.7
PLSE_La	77.4	108.3	80.7	253.7	1407.2
BASL	45.9	90.5	65.7	232.9	1113.0
BASL_La	81.0	85.7	64.2	231.8	1055.1
PRGL_K	59.7	67.6	57.2	216.4	1003.7
TARA	70.7	85.9	61.8	237.8	1067.2
TARA_K	55.6	74.4	56.9	247.8	1108.2
BASL_K	53.3	68.3	58.5	224.4	1045.5
TYDO	73.5	78.0	68.1	198.7	1019.3
SAEX_La	105.2	131.8	111.9	237.6	1485.5
SAGO_K	56.7	74.5	60.0	227.0	1083.6
PHAR	65.6	82.7	62.0	244.5	1113.0
			Ground (reflectance)		
LITTER_K	0.0645	0.0804	0.1063	0.1393	0.1017
LATR_K	0.0626	0.0806	0.1105	0.1482	0.1048
LATR_La	0.0655	0.0838	0.1139	0.1517	0.1082
LITTER	0.0764	0.0988	0.1379	0.1931	0.1309
LATR	0.0740	0.1067	0.1050	0.2140	0.1300
PRGL	0.0487	0.0830	0.0583	0.3225	0.1116
CERE	0.0544	0.1044	0.0484	0.3380	0.1210
SAEX	0.0717	0.1063	0.0796	0.3864	0.1395
SAND	0.2041	0.2645	0.3542	0.3955	0.3320
SAND_K	0.2041	0.2645	0.3542	0.3955	0.3320
SAND_La	0.2041	0.2645	0.3542	0.3955	0.3320
SAEX_K	0.1325	0.1881	0.1961	0.3980	0.2314
PLSE_La	0.0643	0.1242	0.0929	0.4039	0.1627
BASL	0.0508	0.0957	0.0708	0.4066	0.1350
BASL_La	0.0508	0.0957	0.0708	0.0407	0.1350

Table A4. ISTAR color-band data and ground spectroradiometric data for various materials that occur within the flight line zones J, K, and L. Zones are further divided into segments defined by lower case letters (eg., Ja, La). Ground reflectance data were convolved to the band wavelengths of the ISTAR CCD sensors.—Continued.

Zones Jd, K, La	B1	B2	B3	B4	PAN
			Ground (reflectance)—Continued		
PRGL_K	0.0427	0.0797	0.0453	0.4238	0.1185
TARA	0.0462	0.0932	0.0603	0.4243	0.1322
TARA_K	0.0462	0.0932	0.0603	0.4243	0.1322
BASL_K	0.0335	0.0768	0.0470	0.4377	0.1205
TYDO	0.0387	0.0777	0.0386	0.4486	0.1158
SAEX_La	0.0966	0.1407	0.1295	0.4759	0.1844
SAGO_K	0.0374	0.0835	0.0467	0.4952	0.1309
PHAR	0.0459	0.0987	0.0582	0.5215	0.1432

Table A5. ISTAR color-band data and ground spectroradiometric data for various materials that occur within the flight line zones 8, B, C, and D. Ground reflectance data were convolved to the band wavelengths of the ISTAR CCD sensors.

Zones 8, Ba, Cb, and Da	B1	B2	B3	B4	PAN
			Image (digital number)		
tar roof	85.5	76.5	71.3	76.1	730.8
LITTER_8a	80.2	72.3	73.0	89.9	1234.3
Tin_roof1	127.4	118.8	90.7	92.7	965.9
Tin_roof2	130.4	122.7	116.4	131.4	1134.0
med brown soil	117.2	113.6	158.4	166.2	1900.8
PLSE_8a	99.6	107.9	88.1	162.5	1521.5
light brown soil_8a	152.1	156.7	191.4	199.3	2212.3
light brown soil_8b	139.9	148.5	193.8	205.0	2214.0
TARA_Ba	67.6	98.8	72.0	213.5	766.8
PRGL_8a	50.0	60.6	51.5	173.0	1155.1
PRGL_8b	49.4	57.6	50.4	187.5	1141.3
PRGL_Cb	67.8	75.5	59.8	167.4	846.0
SAEX_Cb	85.7	109.9	76.4	229.5	1241.9
SAND_8a	239.5	240.8	240.8	238.6	3090.1
SAND_Cb	237.9	241.9	244.7	244.1	2579.9
SAND_Da	243.5	246.0	246.8	245.8	2782.0
TARA_8a	55.7	67.2	51.5	223.1	1233.7
TARA_Cb	67.1	90.8	62.8	228.9	1038.1
BASL_8a	54.6	64.8	51.1	202.2	1205.2
BASL_8b	43.8	56.9	42.2	238.8	1179.8
BASL_Cb	56.4	74.1	55.0	227.5	897.7
TYDO_8a	45.5	63.0	50.8	235.5	1303.6
TYDO_8b	46.3	55.1	44.0	242.1	1181.8
PHAR_8a	53.4	69.7	50.0	245.4	1326.0

Table A5. ISTAR color-band data and ground spectroradiometric data for various materials that occur within the flight line zones 8, B, C, and D. Ground reflectance data were convolved to the band wavelengths of the ISTAR CCD sensors.—Continued.

Zones 8, Ba, Cb, and Da	B1	B2	B3	B4	PAN
			Ground (reflectance)		
tar roof	0.0611	0.0729	0.0853	0.0981	0.0829
LITTER_8a	0.0645	0.0804	0.1063	0.1393	0.1017
Tin_roof1	0.1046	0.1177	0.1317	0.1413	0.1280
Tin_roof2	0.1220	0.1373	0.1537	0.1649	0.1493
med brown soil	0.1065	0.1446	0.2131	0.2466	0.1966
PLSE_8a	0.0800	0.1200	0.0500	0.2500	0.1700
light brown soil_8a	0.1331	0.1808	0.2664	0.3082	0.2458
light brown soil_8b	0.1331	0.1808	0.2664	0.3082	0.2458
TARA_Ba	0.0296	0.0685	0.0429	0.3221	0.0992
PRGL_8a	0.0487	0.0830	0.0583	0.3225	0.1116
PRGL_8b	0.0487	0.0830	0.0583	0.3225	0.1116
PRGL_Cb	0.0487	0.0830	0.0583	0.3225	0.1116
SAEX_Cb	0.0717	0.1063	0.0796	0.3864	0.1395
SAND_8a	0.2041	0.2645	0.3542	0.3955	0.3320
SAND_Cb	0.2041	0.2645	0.3542	0.3955	0.3320
SAND_Da	0.2041	0.2645	0.3542	0.3955	0.3320
TARA_8a	0.4620	0.0932	0.0603	0.4243	0.1322
TARA_Cb	0.0462	0.0932	0.0603	0.4243	0.1322
BASL_8a	0.0335	0.0768	0.0470	0.4377	0.1205
BASL_8b	0.0335	0.0768	0.0470	0.4377	0.1205
BASL_Cb	0.0335	0.0768	0.0470	0.4377	0.1205
TYDO_8a	0.0387	0.0770	0.0386	0.4486	0.1158
TYDO_8b	0.0387	0.0770	0.0386	0.4486	0.1158
PHAR_8a	0.0459	0.0987	0.0582	0.5215	0.1432

Table A6. Calibration results for the ISTAR. *A*, Blue. *B*, Green. *C*, Red. *D*, Near-infrared-band data with reflectance values ≤0.455. *E*, Near-infrared-band data with reflectance values ≤0.400. *F*, Panchromatic image data for the four regions having ground reflectance data.

A

Zone	N	Multiple R	R square	R square adj.	S.E.	F	Significance F
1b and 2 w/o CEMENT	17	0.9767	0.9540	0.9509	14.22	311.20	1.9×10^{-11}
4 and 5	31	0.9907	0.9815	0.9808	8.29	1539.6	1.09×10^{-26}
Jd, K, and La	23	0.9908	0.9818	0.9810	8.24	1137.6	8.93×10^{-20}
8, Cb and Da	24	0.9881	0.9764	0.9753	9.90	910.45	2.14×10^{-19}

B

Zone	N	Multiple R	R square	R square adj.	S.E.	F	Significance F
1b and 2 w/o CEMENT	17	0.9855	0.9713	0.9693	11.35	507.75	5.56×10^{-13}
4 and 5	31	0.9865	0.9732	0.9723	9.68	1053.88	2.37×10^{-24}
Jd, K, and La	23	0.9943	0.9887	0.9881	6.30	1840.19	6.14×10^{-22}
8, Cb and Da	24	0.9748	0.9503	0.9480	13.52	420.83	7.83×10^{-16}

C

Zone	N	Multiple R	R square	R square adj.	S.E.	F	Significance F
1b and 2 w/o CEMENT	17	0.9949	0.9899	0.9892	6.99	1473.53	2.15×10^{-16}
4 and 5	31	0.9898	0.9797	0.9790	9.90	1400.55	4.22×10^{-26}
Jd, K, and La	23	0.9900	0.9801	0.9791	9.05	1034.96	2.36×10^{-19}
8, Cb and Da	24	0.9880	0.9763	0.9752	10.99	906.43	2.24×10^{-19}

D

Zone	N	Multiple R	R square	R square adj.	S.E.	F	Significance F
1b and 2 w/o CEMENT	17	0.9463	0.8955	0.8860	19.57	94.30	9.90×10^{-07}
4 and 5	31	0.9545	0.9116	0.9073	16.23	235.90	1.39×10^{-13}
Jd, K, and La	23	0.9807	0.9618	0.9594	12.61	403.35	8.97×10^{-13}
8, Cb and Da	24	0.9439	0.8910	0.8858	17.65	171.69	1.41×10^{-11}

E

Zone	N	Multiple R	R square	R square adj.	S.E.	F	Significance F
1b and 2 w/o CEMENT	17	0.9333	0.8711	0.8550	21.61	54.09	7.95×10^{-05}
4 and 5	31	0.9559	0.9137	0.9071	17.47	137.78	2.72×10^{-08}
Jd, K, and La	23	0.9918	0.9837	0.9825	8.74	788.24	5.08×10^{-13}
8, Cb and Da	24	0.9676	0.9363	0.9318	14.43	206.11	9.07×10^{-10}

F

Zone	N	Multiple R	R square	R square adj.	S.E.	F	Significance F
1b and 2 w/o CEMENT	17	0.9916	0.9832	0.9821	97.38	882.19	9.63×10^{-15}
4 and 5	31	0.9881	0.9764	0.9755	100.53	1200.50	3.76×10^{-25}
Jd, K, and La	23	0.9898	0.9797	0.9788	86.67	1017.31	2.82×10^{-19}
8, Cb and Da	24	0.9696	0.9401	0.9374	163.50	345.78	6.06×10^{-15}

Table A7. Calculated gains and offsets for ISTAR image data determined from ground reflectance data for various vegetation and inorganic surface materials acquired during 2000. Gain is in units of DN/ground reflectance; offset is in DN units.

Flight zone set	Blue (gain)	Blue (offset)	Green (gain)	Green (offset)	Red (gain)	Red (offset)	NIR (gain)	NIR (offset)	Pan (gain)	Pan (offset)
1b, 2	1002.3	17	860.7	3	506.5	28	435.1	14	7384.4	270
4, 5a, 5b	1081.6	22	879.4	3	576.3	37	485.8	10	7711.3	353
Jd, K, La	1098.2	17	931.4	1	619.4	31	569.5	3	8021.2	101
8a, 8b, Ba, Cb, Da	1096.9	12	911.6	–1	623.3	28	449.9	–2	8218.6	184
Average	1069.8	17	895.8	2	581.4	31	534.1	5	7833.9	227
	39.5	4	27.4	2	47.1	4	52.3	9	316.3	109

of water, but the different look directions of the four-color charge-coupled devices produced noncoincident sun glint in the four color images, causing the water's surface to appear multicolored (peacock colored), which made it impossible to determine a consistent, unique signature for water in order to easily remove it.

The next mask needed for image analysis was the vegetation mask. This mask was used to restrict the calculation of spatial texture to pixels that are most likely vegetation. This mask was also used to determine the areal density of vegetation at any given location and to restrict the area considered by the final vegetation classifier to make the classification processing faster and more accurate. Several vegetation indices were examined that were shown to have superior accuracy for distinguishing vegetation by Elvidge and Chen (1995), as well as the Spectral Angle Mapper developed by Yuhas and Goetz (1993), and Kruse and others (1993).

Visual examination of bright and dark vegetation units within the training areas showed that the normalized difference vegetation index (NDVI) best separated vegetation from bare ground without omitting dark litter and dark vegetation. However, only the brightest alluvium was eliminated in the attempt to include the dark patches of vegetation, which produced anomalously high texture values along the margins of vegetated and nonvegetated areas. It was difficult to exclude alluvium and include dark vegetation using just the NDVI ratio image. Investigations of methods to exclude the alluvium while not excluding the sparse, dark vegetation (whose flat reflectance pattern is similar to that of alluvium) indicated that the blue band would be effective because alluvium is higher in the blue band than is the dark vegetation. It was also found that an NDVI produced from the NIR and red bands without haze subtraction better isolated the bright and dark vegetation from the alluvium.

Ambiguities for vegetation growing within the alluvium were produced when haze was subtracted from the red and NIR bands without converting the resulting DN to reflectance. Thus, the NDVI ratios were recomputed without subtracting haze, and a blue band parameter was added for the dark NDVI index to separate dark vegetation from alluvium. Both bright and dark vegetation masks were produced because vegetation density was based solely on the density of bright vegetation. These two vegetation masks were used to separate bright and dark vegetated ground within the ISTAR color image data, which was relevant to digital analyses of vegetation characteristics in this study and subsequent classification based on the characteristics. The bright vegetation NDVI ratio is ≥0.153; the dark-vegetation NDVI ratio range is 0.00 to 0.152, if the blue band DN is ≤133.

Vegetation Texture Data

Vegetation at the Genus or Family level have different branch and leaf structure which, viewed from above, appears as textural differences. Manual photographic interpretation uses these textural differences intuitively to map vegetation, but digital classifications of imagery require the image texture to be quantified. There are two categories of digital filters used to detect and quantify texture within image data: occurrence and co-occurrence. Occurrence filters were developed first and represent a pixel's texture by some statistical measure of image data within a specified area centered on that pixel. Co-occurrence filters were later developed by Haralick and others (1973); this category of texture filter looks at the correspondence between a designated image area (boxcar) and an adjacent image area shifted an x and y amount and, as such, represents the spatial dependence of texture (Ferro and Warner, 2002). This type of filter amplifies moderate levels of texture, but has little to no noticeable effect for very smooth or very rough surfaces. There are several types of occurrence and co-occurrence filters; many were tried and it was found that the occurrence variance filter and the co-occurrence contrast and variance filters better separate the vegetation alliances. The contrast (or inertia) filter is the squared difference between the unshifted and shifted pixel values. Filter algorithms within commercial software do not compensate for nondata and, as a result, produce anomalously high texture values along borders between data and nondata. Therefore, new texture algorithms were produced that exclude nondata in their calculation of texture. A textural filter with a circular shape was also produced and tested. This filter was intended

to approximate the appearance of vegetation by excluding internal pixels whose distance from the normal boxcar's center was greater than the boxcar radius plus 0.4.

Davis and others (2002) found that a filter dimension of 10 m worked best for the CRE vegetation. This dimension seemed too large, especially for small vegetation patches. Thus, a range of areal dimensions was examined to determine the most appropriate for alliance separation. The optimum areal dimension for the texture filters was determined by applying a range of filter dimensions to the training areas (locations shown in fig. 10) and determining the filter dimension that best separated the different vegetation alliances. Variance filters applied to the NIR and panchromatic bands showed that (1) the NIR band provided a larger range in texture values within the vegetation because NIR values vary more than panchromatic values in vegetation, and (2) the panchromatic band produced anomalously high texture values on some vegetation borders, which was attributed to the misregistration mentioned previously. Thus, the NIR band data were used for texture.

Examination of the results using co-occurrence and circular occurrence texture filters showed that the contrast and variance co-occurrence filters better separated (≥5% accuracy) the alliances than did other co-occurrence filters and the occurrence variance filter. The circular filters did not significantly improve the results. It was also found that information within alliance delineations was different for two sizes of the co-occurrence filters, a 9-by-9 boxcar (4-m dimension) and a 23-by-23 boxcar (10-m dimension). The larger dimension for texture better smoothed the variations within large stands, but degraded the obvious texture of small stands by including adjacent alliance variations in the small alliances. It is common in classification efforts for forests to use semivariograms of texture showing change in texture with increasing filter dimension. This approach was also investigated using the texture results from this study, but the changes observed were equally represented only by the two co-occurrence dimensions listed above, and only these two dimensions of the variance and contrast filters were used in this classification in order to reduce the processing time.

Vegetation Areal Density

Certain vegetation alliances may be separated by the areal density of vegetation in the areas where they commonly occur. In order to test and use this parameter, an areal vegetation density database was constructed using an adaptive filter developed by Schwartz and Soha (1977) that uses only the image data around the DN of a particular pixel. This filter minimizes border smearing between densely and sparsely vegetated areas. Two filters of different sizes were employed. The smaller filter examines the very local areal density around a pixel; the larger filter examines the data produced by the smaller filter to determine pixels with similar densities and uses only these pixels within its areal dimension to calculate vegetation density. The bright vegetation mask produced previously was used by these filters to determine the presence of vegetation. It was found that a small 5-by-5 filter (2.2-m dimension) and a large 17-by-17 filter (7.5-m dimension) provided good separation between some vegetation alliances with respect to their areal vegetation density.

Preclassification Results

In preparation for the corridorwide data classification, the accuracies obtained on groundtruth regions using various combinations of the above databases were examined. It appeared that (1) four-band data produced higher mapping accuracies than their ratios, (2) inclusion of texture with band data increased mapping accuracies by 10%–25%, (3) the use of all four-texture measures produced higher mapping accuracies than any subset of the four-texture measures, (4) vegetation density did not increase mapping accuracy over that provided by the four ISTAR bands and four-texture measures, and (5) mapping accuracies for the groundtruth regions using the band and texture data ranged from 65%–95% within various groundtruth areas. The lower accuracies were primarily due to misclassification of *Tamarix* (TARA) and *Prosopis-Acacia* (PRGL), even though bright and dark training areas were separated for these two classes to decrease classifier confusion. This step showed that acceptable overall producer accuracies could be obtained from any particular training site, but accuracy might degrade when all training areas are considered in a single corridorwide classification.

Image Data Classification

Maximum likelihood classification was then performed on the same combinations of data used above, but operated on all groundtruth areas using the image mosaic of all groundtruth regions to determine which data provided the highest mapping accuracy for corridorwide mapping. This total groundtruth classification analysis produced the same conclusions using the different database combinations as those obtained from individual training sites. Thus, only the four ISTAR bands and the four-texture measures were used in the final vegetation classification processing. The overall producer mapping accuracy resulting from the integrated classification was only 45%–50%, but many of the vegetation alliances had accuracies of 75%–90%.

Results from confusion matrix analysis were used to determine the sources of the inaccuracies (misclassification) for specific alliances. The training data for those alliances were revised using the n-D visualization tool provided by ENVI (ITT Visual Information Solutions©, 2006), which allows interactive editing of alliances clusters in n-space. This editing was performed in a stepwise manner, changing the groundtruth area for just a single alliance before rerunning the classifier and examining its results. This stepwise process minimized changes in groundtruth and provided a better

understanding of the results produced by each change. The overall producer accuracy after groundtruth editing was 84%, but this accuracy is only related to the groundtruth regions. Mapping accuracy needs to be established using randomized field verification of the results. Thus, a set was developed of stratified random sample locations for each vegetation unit within each subzone of the CRE, and the classification results at these points were field checked.

References

Davis, P.A, Staid, M.I, Plescia, J.B., and Johnson, J.R., 2002, Evaluation of airborne image data for mapping riparian vegetation within the Grand Canyon: U.S. Geological Survey Open-File Report 02-470, 65 p.

Elvidge, C.D., and Chen, Z., 1995, Comparison of broad-band and narrow-band red and near-infrared vegetation indices: Remote Sensing of Environment, v. 54, p. 38–48.

ENVI Image Analysis Software, 2006, v4.2, ITT Visual Information Solutions©: Boulder, Colo.

Ferro, C.J.S., and Warner, T.A., 2002, Scale and texture in digital image classification: Photogrammetric Engineering and Remote Sensing, v. 68, p. 51–63.

Haralick, R.M., Shanmugam, K., and Dinstein, I., 1973, Textural features for image classification: IEEE Trans. On Systems, Man and Cybernetics SMC–3, p. 610–621.

Kruse, F.A., Lefkoff, A.B., Boardman, J.G., Heidebrecht, K.B., Shapiro, A.T., Barloon, P.J., and Goeta, A.F.H., 1993, The Spectral Image Processing System (SIPS)—interactive visualization and analysis of imaging spectrometer data: Remote Sensing of Environment, v. 44, p. 145–163.

Schwartz, A.A., and Soha, J.M., 1977, Variable threshold zonal filtering: Applied Optics, v. 16, p. 1779–1781.

Yuhas, R.H., and Goetz, A.F.H., 1993, Comparison of airborne (AVIRIS) and spaceborne (TM) imagery data for discriminating among semi-arid landscape endmembers: Proceedings, Ninth Thematic Conference on Geologic Remote Sensing, Pasadena, Calif., Feb. 8–11, Environmental Research Institute of Michigan, p. 503–511.